NRC Research and Technical Assistance Report

INTERIM REPORT

5-30-79

Accession No. _____

Contract Program or Project Title: Code Assessment and Applications Program

Subject of this Document: Comparison of RELAP4/MOD6 to THTF Test 177

Type of Document: Code Assessment and Applications report

Author(s): C. B. Davis

Date of Document: May 1979

Responsible NRC Individual and NRC Office or Division: W. C. Lyon, NRC-RSR

Kay Rose
H. F. Pearson, Supervisor
Information Processing
EG&G Idaho, Inc.

Prepared for
U.S. Nuclear Regulatory Commission
Washington, D.C. 20555

NRC Fin #A6047

INTERIM REPORT

NRC Research and Technical Assistance Report

CAAP-TR-049
FOR U.S. NUCLEAR REGULATORY COMMISSION

CODE ASSESSMENT AND APPLICATIONS PROGRAM

COMPARISON OF RELAP4/MOD6 TO THTF TEST 177

By
C. B. Davis

May 1979

EG&G Idaho, Inc.

IDAHO NATIONAL ENGINEERING LABORATORY

DEPARTMENT OF ENERGY

IDAHO OPERATIONS OFFICE UNDER CONTRACT EY-76-C-07-1570

EG&G Idaho, Inc.

FORM EG&G-398
(Rev. 12-78)

INTERIM REPORT

Accession No. _____

Report No. CAAP-TR-049

Contract Program or Project Title: Code Assessment and Applications Program

Subject of this Document: Comparison of RELAP4/MOD6 to THTF Test 177

Type of Document: Code Assessment and Applications report

Author(s): C. B. Davis

Date of Document: May 1979

Responsible NRC Individual and NRC Office or Division: W. C. Lyon, NRC-RSR

This document was prepared primarily for preliminary or internal use. It has not received full review and approval. Since there may be substantive changes, this document should not be considered final.

EG&G Idaho, Inc.
Idaho Falls, Idaho 83401

Prepared for the
U.S. Nuclear Regulatory Commission
and the U.S. Department of Energy
Idaho Operations Office
Under contract No. EY-76-C-07-1570
NRC FIN No.

A6047

INTERIM REPORT

CAAP-TR-049
May 1979

COMPARISON OF RELA /MOD6 TO THTF TEST 177

by

C. B. Davis

ABSTRACT

The ability of the RELAP4/MOD6 computer code to predict the behavior of a pressurized water reactor core during the blowdown phase of a loss-of-coolant accident was assessed. Predictions of a core component model were compared with data from a Thermal-Hydraulic Test Facility blowdown experiment.

SUMMARY

This report describes an assessment of the ability of the RELAP4/MOD6 computer code to predict the behavior of an LPWR (large pressurized water reactor) core during the blowdown phase of a loss-of-coolant accident. As part of the assessment process, predictions of a core component model were compared with data from THTF (Thermal-Hydraulic Test Facility) Test 177. The THTF is designed for separate-effects testing of an electrically heated rod bundle which simulates an LPWR core. Test 177 simulated the core thermal-hydraulic response during a blowdown initiated by a 200% cold leg break. The test was conducted from an initial pressure of 15.9 MPa, a core inlet temperature of 550 K, and core power of 3.7 MW.

Test 177 was performed especially for use in the independent assessment of RELAP4/MOD6 and was conducted with significantly different initial and transient boundary conditions from tests used in previous assessment comparisons. A prediction of Test 177 was made using a RELAP4 core component model which was driven with measured initial and boundary conditions. The prediction was made without knowledge of the measured core response and thus was a "blind" prediction. This report compares the predictions with measured data. The comparisons are summarized below.

Most cladding temperature measurements increased suddenly at about 1 s after rupture, denoting the occurrence of CHF (critical heat flux). Measured cladding temperatures decreased suddenly at about 2 s after rupture denoting the occurrence of a rewet. This rewet started at the top of the core and propagated downward through much of the core. A second CHF occurred near 4 s after rupture. The trends in predicted cladding temperatures were similar to those observed during the test. In particular, the rewet at 2 s and CHF at 4 s were

predicted. Predicted cladding temperatures were generally within the range of the corresponding measured temperatures during the blowdown. Predicted and measured peak cladding temperatures were 820 and 895 K, respectively. The predicted peak cladding temperature was within 5 K of the maximum of the average measured temperature at the peak power step. Cladding temperatures were predicted well throughout the core.

CONTENTS

303 353

FIGURES

FIGURES (Cont'd)

TABLES

I. INTRODUCTION

This study represents a portion of the initial effort to apply independent assessment techniques to the RELAP4/MOD6, Update 4[(a)] computer code. Independent Code Assessment is a new field of study and is just now being developed into a structured process. Therefore, the objectives of this study were twofold:

(1) To explore and develop optimum techniques, rules and guidelines for performing independent assessment of codes.

(2) To apply the preceding techniques, rules and guidelines to the RELAP4/MOD6, Update 4 code in order to gain insight into what constitutes a successful (or unsuccessful) independent assessment and to gain further knowledge about the quality of the subject code.

One of the first steps in this process is to develop a matrix (Table I) identifying the complete scope of effort. As shown in Table I, that scope includes analyses of component, system and integral blowdown and reflood phenomena. The studies described in this report are those identified as Subtask 15 in Table I and specifically address core component blowdown heat transfer and hydraulic effects.

The approach taken in each study's base run was to formulate a firm set of ground rules prior to all analysis. These ground rules covered modeling techniques, code option selection, the code user input values and were based on the best, published information from all previous developmental assessment. The use of a fixed set of ground

---

(a) This code is filed under Configuration Control No. C0010006 at the INEL Computer Science Laboratory. Associated steam tables are on file under the identification number H0020178 at the same facility. The code actually used was identical to RELAP4/MOD6, Update 4 except that an update was used to allow plotting of internal heat slab temperatures.

303 357

TABLE I

MATRIX FOR CODE ASSESSMENT

OF RELAP4/MOD6

	EXPERIMENTS SELECTED	FEATURES EVALUATED								
		BLOWDOWN HEAT TRANS. & HYDRAULICS	REFLOOD HEAT TRANS. AND HYDRAULICS	FUEL BEHAVIOR	SCALING EFFECTS	DIFFERENT SYSTEMS	TEST PREDIC-TION	COMPONENT EFFECTS	SYSTEMS EFFECTS	INTEGRAL EFFECTS
1. SEMISCALE, THTF CORE BLOWDOWN	SEMISCALE S-06-5, THTF 105	X				X		X		
2. SEMISCALE, LOFT PRESSURIZER BLOWDOWN	SEMISCALE S-04-4, S-06-5, LOFT L1-4				X	X		X		
3. SEMISCALE, LOFT STEAM GENERATOR BLOWDOWN	SEMISCALE S-01-4A, S-06-5, LOFT L1-4				X	X		X		
4. STANDARD PROB. 7 LOFT L1-4	LOFT L1-4						X		X	
5. SEMISCALE, LOFT ISOTHERMAL COMP.	SEMISCALE S-01-4A, LOFT L1-4				X	X			X	
6. SEMISCALE, FLECHT CORE REFLOOD	SEMISCALE S-03-D, FLECHT LFR 4019, 11003		X			X		X		
7. SEMISCALE, FLECHT-SET, PKL COMP.	SEMISCALE S-03-5 FLECHT-SET 2714B PKL K5A		X		X	X			X	
8. PKL PREDICTION	PKL K5A		X				X		X	
9. SEMISCALE INTEGRAL EXPERIMENTS (6)	SEMISCALE S-04-5, S-04-6, S-06-1, S-06-2, S-06-5, S-06-6	X	X						X	X
10. MARVIKEN CRITICAL FLOW TESTS	TBD				X			X		
11. SEMISCALE MOD-3 BLOWDOWN	SEMISCALE S-07-1	X				X	X		X	
12. SEMISCALE MOD-3 REFLOOD	SEMISCALE S-07-4		X			X	X		X	
13. SEMISCALE MOD-3 INTEGRAL	SEMISCALE S-07-6	X	X			X	X		X	X
14. PBF LOCA SERIES	LOC-11, LOC-3	X		X				X		
15. ADDITIONAL THTF TEST (Extension to Subtask 1)	THTF 177	X					X	X		
16. LOFT L1-5 PREDICTION	LOFT L1-5						X		X	
17. ADDITIONAL SEMISCALE, FLECHT CORE REFLOOD (Extension to Subtask 6)	SEMISCALE S-03-A FLECHT LFR 2414, 13404, 13609		X			X		X		
18. ADDITIONAL SYSTEM REFLOOD TESTS (Extension to Subtask 7)	SEMISCALE S-03-8, FLECHT-SET 2213B PKL K7A		X		X	X			X	

303 358

rules was necessary to provide consistency between the several blowdown and reflood gravity and forced feed studies. However, additional studies were made subsequent to these base runs. In certain fruitful areas, further diagnostic analyses were performed to clarify the prior results. These analyses are clearly identified as Additional Studies.

The results of this study are important because:

(1) They provide insight as to steps required for the successful independent assessment of a code.

(2) They identify some of the capabilities and deficiencies of the RELAP4/MOD6, Update 4 code within the framework of independent assessment.

(3) They advance the state-of-the-art of the code input selection process on which the success of PWR-event prediction depends.

THTF (Thermal-Hydraulic Test Facility) data were used to analyze the capability of RELAP4 to calculate the blowdown response of a core component. Section II of this report presents descriptions of the THTF, experiment, and pertinent instrumentation and measurement accuracy.

Section III describes the computer model nodalization, code options, and method of applying boundary conditions.

Section IV describes results and specific conclusions drawn from the base run.

An additional study investigating the sensitivity of the results to input boundary conditions is described in Section V.

The general conclusions drawn for the total study and recommendations for future code application derived therefrom are given in Section VI.

303 359

II. EXPERIMENTAL FACILITY

The THTF program is an experimental separate effects study of the thermal-hydraulic response of a simulated PWR core during the blowdown portion of a loss-of-coolant experiment.

1. FACILITY DESCRIPTION

Figure 1 shows a schematic of the THTF. The system contains a vessel, pump, pressurizer, heat exchangers, pressure-suppression system, and piping. The vessel contains a core simulator, upper and lower plenums, and downcomer.

The core simulator in the THTF contains 49 electrically heated rods. The diameter and heated length of the rods are 0.0107 and 3.66 m, respectively. A cosine axial power distribution is simulated by nine power steps in the heater rods. The power profile is radially uniform within the core. Figure 2 shows the relative location of the grid spacers, thermocouple levels, and power steps in the core. A more detailed description of the THTF may be found in Reference 1.

2. EXPERIMENT DESCRIPTION

THTF Test 177[2] was performed especially for use in the independent assessment of RELAP4/MOD6. Consequently, the initial and transient boundary conditions for Test 177 were considerably different from the tests used in previous assessment studies[3,4]. The initial conditions of Test 177, shown in Table II, are representative of a typical[5] commercial PWR (Zion I). The Zion I plant is a Westinghouse four-loop PWR of the 15x15 bundle design.

303 360

TABLE II

COMPARISON OF INITIAL CONDITIONS OF TEST 177 AND A TYPICAL PWR

Parameter	Test 177	Typical PWR
System pressure (MPa)	15.9	15.7
Total Power (MW_t)	3.697	3238
Maximum linear heat generation rate (kW/m)	37.3	35.8
Core coolant mass flux ($kg\ s^{-1}\ m^{-2}$)	3610	3670
Core coolant inlet temperature (K)	550	550
Core coolant outlet temperature (K)	583	583

303 361

Test 177 was conducted so that the core thermal-hydraulic response was similar to the calculated response[5] of the Zion I core during a blowdown initiated by a 200% cold-leg break.

Four heater rods were unpowered during Test 177.

3. MEASUREMENTS AND ACCURACY

The THTF measurements used to drive the RELAP4 component model or to compare with predictions are described in Table III. Measurement standard deviations, based on the data report[2], are also presented. These standard deviations do not include uncertainty associated with nonhomogeneous, transient, two-phase flow and thus must be considered rough estimates.

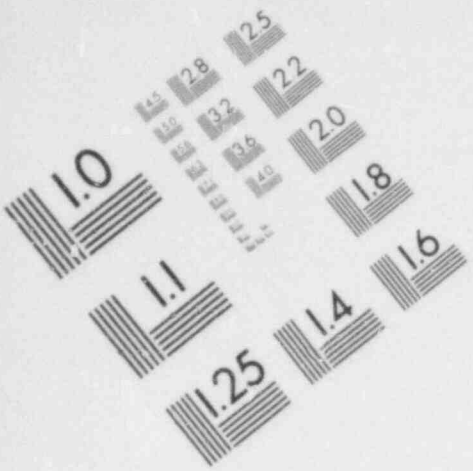

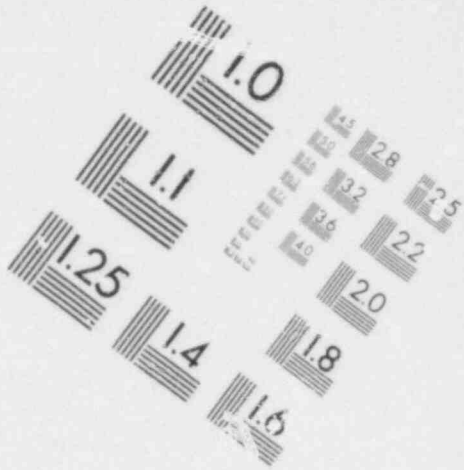

IMAGE EVALUATION
TEST TARGET (MT-3)

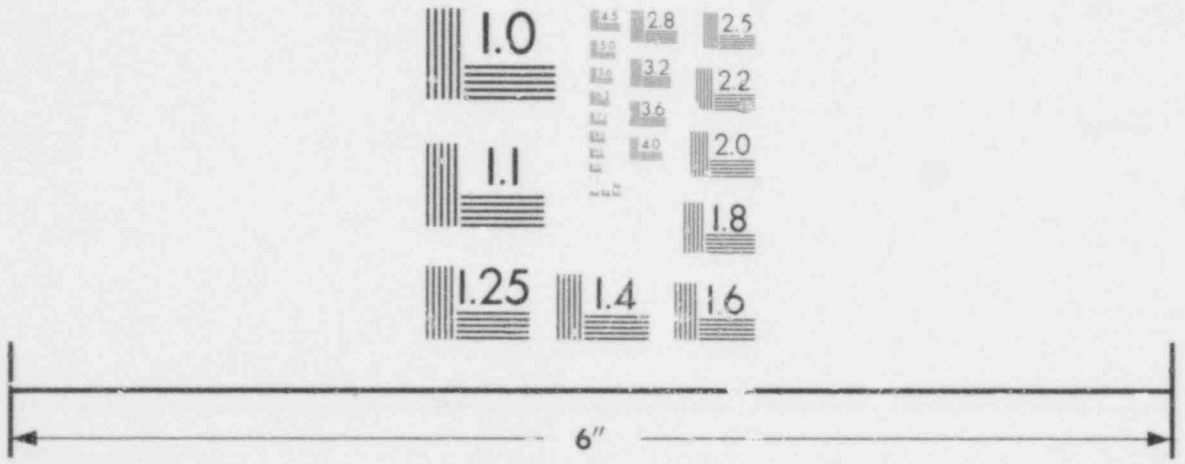

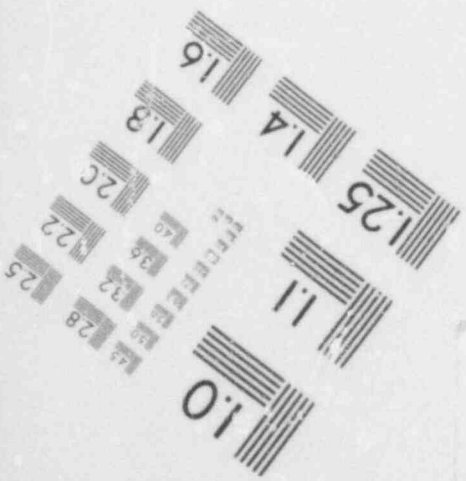

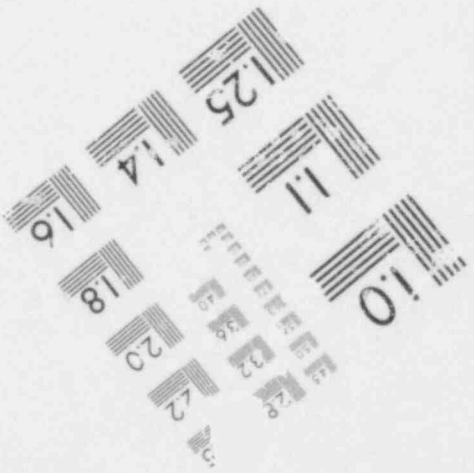

TABLE III

SUMMARY OF THTF MEASUREMENTS

Measurement	Instrument Designation[a]	Estimated Standard Deviation
Volumetric Flow (Turbine Meter)		
Vertical Inlet Spool Piece	FE-166	9×10^{-4} m^3/s[b]
Vertical Outlet Spool Piece	FE-216	8×10^{-4} m^3/s[b]
Density (Gamma Densitometer)		
Vertical Inlet Spool Piece	DE-168	12.9 kg/m^3 @ 961 kg/m^3
Vertical Outlet Spool Piece	DE-218	12.9 kg/m^3 @ 961 kg/m^3
Pressure (Strain Gauge)		
Horizontal Inlet Spool Piece	PE-26	55 kPa
Differential Pressure (Strain Gauge)		
Across Core	PDE-200	5 kPa
Temperature (Chromel/Alumel Thermocouple)		
Bundle Inlet	TE-151	2.4 K
Bundle Outlet Subchannel	------	2.4 K
Heater Rods	------	2.4 K

(a) Instrument designations are consistent with the nomenclature of the THTF data reports.

(b) In addition to this standard deviation, the turbine meters have a dead band between ± 0.005 m^3/s.

304 001

III. BASE RUN MODEL

The base run for this study is the "blind" prediction of Test 177 which is described in Reference 6. The model used in the prediction is stored under INEL Configuration Control No. H00836IB.

1. NODALIZATION

Figure 3 shows the RELAP4 model of the THTF vessel used in the prediction. The model simulates the active core plus all the primary system between the core and nearest flow measurements.

The RELAP4 model is basically the same model as used in a previous independent assessment data comparison[3]. The core, represented by volumes 13 through 21, is modeled axially with one volume per power step. The lower and upper plenums are each modeled as single volumes. The vertical inlet and outlet spool pieces, represented by volume 1 and 24 respectively, house the fluid flow and density measuring devices.

The 45 active heater rods are modeled with heat slabs 1 through 9. The 4 unpowered heater rods are modeled with heat slabs 37 through 45. The unheated lengths of the rods are modeled with heat slabs 10, 21, and 33. The core barrel is modeled with heat slabs 11 through 19 and 22. The vessel is modeled with heat slabs 20, 23 through 31, and 34. Piping was modeled with heat slabs 32, 35, and 36.

2. CODE OPTIONS

The following code options and/or correlations were applied in the prediction:

(1) Core heat transfer was calculated with the default and/or recommended options of RELAP4/MOD6, Update 4[7]. Specifically the HTS2 heat transfer surface was used. CHF was calculated with the recommended CHF correlations[b]. Transition boiling was calculated with the modified Tong-Young correlation. Film boiling was calculated with the Condie-Bengston III film boiling correlation.

(2) The vertical slip model was not used in the core. The vertical slip model, with default coefficients[7], was applied in the downcomer.

(3) The bubble rise option was not used.

(4) The compressible form of the momentum equation was used at all junctions.

(5) The enthalpy transport model was used to initialize the core model but was not used during the transient calculations.

3. BOUNDARY CONDITIONS

Measured boundary conditions of core power, fluid flow, and fluid state were applied to the RELAP4 model. Figure 4 shows the normalized core power history input to the model. The core power reaches a minimum at 1.9 s, begins to increase, rapidly climbs to 60 percent of initial power by 4.7 s and finally drops to zero by 10.2 s.

(b) The recommended CHF correlations are the W-3 correlation for the subcooled regime, Hsu and Beckner's modified W-3 correlation for the saturated high flow regime, and Smith and Griffith's modified Zuber correlation for the saturated low flow regime.

Figure 5 shows the fluid pressure input in the vertical inlet spool piece. The input was based on PE-26[c] which is the pressure measurement nearest to the vertical inlet spool piece. The pressure drops from 15.9 to 9.2 MPa during the first 0.15 s of blowdown. The remainder of the depressurization occurs at a much lower rate and shows a significant change in depressurization rate only between 4.5 and 5.5 s.

Figure 6 shows the mass flow rate input to the model at the vertical outlet spool piece. Positive flow denotes mass leaving the system. The input flow decreased rapidly, reversed at 1.5 s indicating flow into the vessel, and resumed an outward flow direction at 2.8 s. The flow remained out of the system until 14.7 s when the last major flow reversal occurred. The input flow was based on the Aya model during the first 3 s of blowdown and the homogeneous model afterwards. The Aya model combines the readings of a densitometer, drag disk, and turbine meter to calculate the mass flow rate of each phase, slip velocity, and the total mass flow rate. The homogeneous model combines the readings of the turbine meter (FE-216) and densitometer (DE-218) to calculate mass flow rate by assuming a homogeneous fluid.

(c) Instrument designations are consistent with the nomenclature of the data report. Figure 1 shows instrument locations.

IV. BASE RUN RESULTS

The base run for this study is the "blind" prediction of Test 177 and is documented in Reference 6. The prediction was made with the model described in Section III. Figures 5 through 14 illustrate fluid behavior during the test. Figures 15 through 25 show predicted and measured heater rod cladding temperatues.

Figures 6 and 7 illustrate the fluid behavior at the vertical outlet spool piece. The mass flow, which was input to the model, was generally positive (out of the vessel) during the test as shown in Figure 6. Figure 7 shows predicted and measured fluid density. (This prediction is independent of the input fill junction enthalpy when the flow is out of the vessel). The deviation between predicted and measured density is usually less than the measurement uncertainty (see Table II) except for the sudden reduction in measured density between 3 and 4 s and after 15 s. The flow at the vertical outlet spool piece after 15 s was into the vessel and the density of the entering fluid was based on the measurement shown in Figure 7. The discrepancy between predicted and measured density after 15 s is due to the comparison of a point measurement with a volume-averaged prediction.

Figures 8 and 9 illustrate the fluid behavior at the vertical inlet spool piece during the test. Figure 8 compares predicted and measured volumetric flow. The measured flow was initially positive, denoting flow into the vessel, reversed immediately following rupture, and was nearly steady from 1 to 4 s. The prediction follows the general trends of the measurement. However, signficantly too much flow was predicted between 1.5 and 4 s. This overprediction can be partially explained by uncertainty in the flow input to the model at the vertical outlet spool piece and will be discussed in Section V.

Figure 9 compares calculated and measured fluid density in the vertical inlet spool piece[(d)]. In the test, this fluid remained subcooled until 3.9 s after rupture when saturated fluid, which originated in the core, entered the spool piece causing a sharp decrease in density. Saturated fluid was predicted to reach the spool piece about 1 s earlier than measured because the fluid velocity was overpredicted between 1.5 and 3 s (see Figure 8). After saturated fluid reached the spool piece, both predicted and measured density decreased to nearly vapor density.

Figures 10 and 11 show predicted fluid mass flow rate and quality in the center of the core. The figures show only predictions since these parameters were not measured. The predicted mass flow follows the trends of the flow input at the vertical outlet spool piece (see Figure 6). The predicted mass flow rate was initially positive, indicating flow up through the core, reversed immediately after rupture, and reached a negative maximum at 0.5 s. By 1.0 s, the flow had stagnated. A significant amount of flow down through the core was predicted between 1.5 and 4 s. Figure 8 shows that during this time too much flow through the vertical inlet spool piece was predicted. Consequently, too much flow was also probably predicted through the core between 1.5 and 4 s. Significant positive flow was predicted between 5 and 7 s. The predicted fluid quality, shown in Figure 11, was strongly influenced by the predicted flow rate. When the predicted flow rate was large, the predicted quality was relatively low; when the flow rate was small, the predicted quality was relatively high.

(d) The vertical inlet spool piece is modeled with a time-dependent volume where the density is input based on measurement. The prediction shown in Figure 9 corresponds to the volume adjacent to the spool piece. The prediction is independent of the input density when the flow is out of the vessel which is usually the case.

Figure 12 shows predicted and measured differential pressure across the core. The predicted differential pressure follows the trends of the predicted core mass flow rate which is shown in Figure 10. The large amount of flow predicted down through the core between 1.5 and 4 s corresponds to a predicted large negative differential pressure. The positive core flow between 5 and 7 s is also reflected in the predicted differential pressure. The predicted differential pressure agrees relatively well with the measurement except between 1.5 and 4 s. The results shown in Figures 8 and 12 indicate that too much flow was predicted down through the core between 1.5 and 4 s after rupture.

Figure 13 shows predicted fluid temperature near the bottom of the core with a typical measurement. Both predicted and measured fluid temperature increased rapidly from 0.4 to 1 s after rupture due to the flow of warmer fluid down through the core towards the cold leg break. The accurate prediction of the time of the temperature increase indicates that the flow through the core was predicted accurately during the first 1 s of the test. After 1 s, both prediction and measurement followed the saturation line.

Figure 14 shows fluid temperature predicted near the top of the core with the mean and range[e] of eight temperature measurements. The data usually followed the saturation line except between 9 and 12 s after rupture when most, not all, of the measurements indicated that the fluid was superheated. The fluid was predicted to remain saturated during the test. However, at 12 s the predicted quality near the top of the core was 95% which indicates that superheat was almost predicted. Thus, the prediction agreed relatively well with measurements.

(e) The range is the region between the minimum and maximum measured temperature.

Figures 15 through 25 compare predicted and measured cladding temperatures. Each figure shows the prediction and the mean and range of temperature measurements at a particular thermocouple level in the core. The distance of the thermocouple level from the BHL (beginning of the heated length) is shown in each figure. Figure 2 shows relative locations of thermocouple levels in the core.

Figure 15 compares predicted and measured cladding temperatures at Level D. Level D is located at 0 94 m from the BHL and is the lowest thermocouple level in the core. Multiple occurrences of CHF followed by rewet were predicted and measured. The initial CHF, defined by a sudden temperature rise in the mean measured temperature, occurred at 1.5 s after rupture and was followed by a rewet, defined by a sudden temperature decrease, 1.5 s later. Cladding temperature measurements indicate that this rewet started near the top of the core and propagated downward. The initial CHF was predicted at 1 s after rupture, followed by a predicted rewet 0.7 s later. The predicted rewet at 1.7 s was caused by the large amount of flow predicted down through the core at this time (see Figure 10). This predicted rewet may be somewhat fortuitous since there is evidence (see Figures 8 and 12) that too much core flow was predicted at this time. Both the prediction and the data mean indicated a second CHF at about 4 s which occurred as the core flow stagnated simultaneously with a power increase (see Figures 10 and 4). A second rewet occurred in both the prediction and experiment at 5.2 s. This rewet was apparently caused by the flow of low-quality fluid from the lower plenum into the core (see Figures 10 and 11). A final CHF was predicted at 6.5 s but was not observed in the experiment. Figure 15 shows that the maximum predicted cladding temperature at Level D was within 15 K of the maximum value of the data mean and was within the data range.

Figure 16 shows predicted and measured cladding temperatures at Level E. The temperatures are similar to those observed at Level D but are generally higher because of the higher axial power peaking factor at Level E. The initial CHF and rewet were predicted slightly earlier than measured. A second CHF caused by flow stagnation and/or power increase (see Figures 10 and 4) was predicted and measured at about 4 s

after rupture. Upflow from the lower plenum at 5.2 s, which caused a rewet at Level D, caused a rewet at Level E in the test but did not cause a rewet in the prediction. The maximum predicted cladding temperature at Level E was 70 K higher than the maximum value of the data mean but was within the data range.

Figures 17, 18, and 19 show predicted and measured cladding temperatures at the bottom, center, and top of the peak power step (Levels F, G, and H, respectively). The temperature response shown in the figures is similar to that observed at Level E except that the mean measured temperatures did not indicate a rewet after 5 s. Predicted and measured peak cladding temperatures in Test 177 occurred at the peak power step at 10 s after rupture. Predicted and measured peak cladding temperatures were 820 and 895 K respectively. The mean measured cladding temperature at Levels F, G, and H at 10 s after rupture was 820 K which is in excellent agreement with the prediction. The predicted cladding temperature remained within the range of measurements during the predicted 20 s of blowdown.

Figures 20 and 21 show predicted and measured cladding temperatures at Levels I and J, respectively. Two occurrences of CHF were predicted and measured. The predicted cladding temperature was within the range of measured data at both levels during the entire test.

Figures 22 and 23 show predicted and measured cladding temperatures at Levels K and L, respectively. The results are similar to those shown previously except that a rewet, which was not predicted, occurred at Level L at 6 s after rupture. Consequently, cladding temperatures at Level L were overpredicted by as much as 90 K after 6 s.

Figure 24 compares predicted and measured cladding temperatures at Level M. CHF was predicted and measured at 5 s after rupture. A rewet, which was not predicted, occurred at 6 s in the experiment. Consequently, cladding temperature was overpredicted by as much 60 K after 6 s.

Figure 25 compares predicted and measured cladding temperatures at Level N, which is the highest thermocouple level in the active core. Cladding temperatures were slightly overpredicted after 6 s.

Figure 26 summarizes the comparison of predicted and measured cladding temperatures. The figure shows the maximum temperature measured by each cladding thermocouple during the blowdown versus the corresponding maximum predicted temperature. The predicted maximum temperatures were usually near the middle of the data and were always within the data range. Based on the results shown in Figures 15 through 26, cladding temperatures were predicted well throughout the core during Test 177.

V. ADDITIONAL STUDY

As described in Section IV, the blind prediction compared favorably with Test 177 data except that too much flow was predicted at the vertical inlet spool piece between 1.5 and 4 s (see Figure 8). This overprediction in flow at the vertical inlet spool piece appears to be partially caused by the boundary conditions applied at the vertical outlet spool piece. Between 1.5 and 2.3 s, the mass flow rate input to the model at the vertical outlet spool piece was probably inaccurate because the turbine meter reading was inside the dead band of the meter. Furthermore, a sharp reduction in fluid density at the vertical outlet spool piece was measured between 3 and 4 s but was not predicted (see Figure 7). Since the mass flow rate was input to the model, the overprediction in fluid density between 3 and 4 s caused an underprediction in the volumetric flow out the vertical outlet spool piece. This underprediction in volumetric flow at the vertical outlet spool piece is partially responsible for the overprediction in flow at the vertical inlet spool piece shown in Figure 8.

An additional RELAP4 run(f) was made to determine the sensitivity of the predicted results to the input boundary conditions. The input for this run was identical to the blind prediction except for the mass flow rate at the vertical outlet spool piece. (Figure 27 shows the flow rate used in each run). The mass flow rate input in the additional run was identical to the one used in the prediction except for two changes. First, the mass flow rate input between 1.5 and 2.3 s was adjusted by assuming a volumetric flow equal to the positive edge of the turbine meter dead band. (Table III shows that the positive edge of the dead band is estimated to be 0.005 m^3/s). Second, the

---

(f) The input for this run has been stored under Configuration Control Number H003184B.

input mass flow rate was adjusted to account for the error in the predicted density (see Figure 7) between 3 and 4 s. The adjustment forced the calculated volumetric flow to equal the measurement between 3 and 4 s. Thus, the adjustment was equivalent to driving the model with the measured volumetric flow, rather than mass flow, between 3 and 4 s.

Figure 28 shows calculated and measured volumetric flow rates at the vertical inlet spool piece. The figure shows that the adjustments to the input mass flow at the vertical outlet spool piece accounted for most of the discrepancy between the prediction and measurement between 1.5 and 4 s.

Figure 29 shows calculated and measured fluid density at the vertical inlet spool piece. The adjustments to the input mass flow rate improved the time at which saturated fluid was calculated to reach the spool piece resulting in an improved density calculation.

Figure 30 shows the effect of the adjustments in input mass flow rate on calculated cladding temperatures at the peak power step. The flow adjustments affected the calculated rewet at 1.5 s and increased the calculated peak cladding temperature by 40 K. The effect of the flow adjustments on calculated cladding temperatures at other power steps was generally less than 20 K.

Based on the results shown in Figures 28 and 29, most of the discrepancies between predictions and measurements at the vertical inlet spool piece can be explained by uncertainty and/or errors in the application of boundary conditions at the vertical outlet spool piece. Predicted cladding temperatures are not sensitive to the uncertainty in the input boundary conditions.

VI. CONCLUSIONS

1. *The RELAP4 prediction adequately represented the hydraulics of Test 177.*

   As described in Section IV, the trends of the data were generally predicted correctly. However, the flow through the vessel was probably overpredicted between 1 and 4 s after rupture (see Figures 8 and 12). Most of this overprediction in flow can be explained by uncertainty in the input boundary conditions as described in Section V.

2. *Heater rod cladding temperatures were predicted well.*

   The time to CHF was predicted accurately throughout the core. A predicted rewet, shown in Figure 19, was similar to a rewet which occurred in the experiment. The maximum temperature predicted to occur at each power step during the test was generally close to the maximum value of the corresponding data mean and within the data range. Predicted cladding temperatures were not sensitive to the uncertainty in the flow boundary conditions.

3. *The RELAP4 model used to make the prediction of Test 177 is suitable for future THTF data comparisons or predictions.*

VII. REFERENCES

1. Project Description ORNL PWR Blowdown Heat Transfer Separate Effects Program Thermal-Hydraulic Test Facility (THTF), ORNL/NUREG/TM-2 (February 1976).

2. V. D. Clemons et al, PWR Blowdown Heat Transfer Separate Effects Program Thermal-Hydraulic Test Facility Experimental Data Report for Test 177, TN-295, to be published.

3. C. B. Davis, Comparisons of RELAP4/MOD6 With Core Blowdown Data, EG&G Idaho, Inc., CVAP-TR-78-012 (May 1978).

4. C. B. Davis, RELAP4/MOD6 Comparison with PWR-BDHT Test 103 Core Data, EG&G Idaho, Inc., PG-R-77-27 (July 1977).

5. G. W. Johnsen et al, A Comparison of "Best Estimate" and "Evaluation Model" LOCA Calculations: The BE/EM Study, EG&G Idaho, Inc, PG-R-76-009 (December 1976).

6. EG&G Internal Letter, R. R. Schultz to T. R. Charlton, Code Assessment Prediction of the Thermal Hydraulic Test Facility Test 177, RRS-1-79, January 17, 1979.

7. RELAP4/MOD6 A Computer Program for Transient Thermal-Hydraulic Analysis of Nuclear Reactors and Related Systems User's Manual, CDAP TR003 (January 1978).

304 014

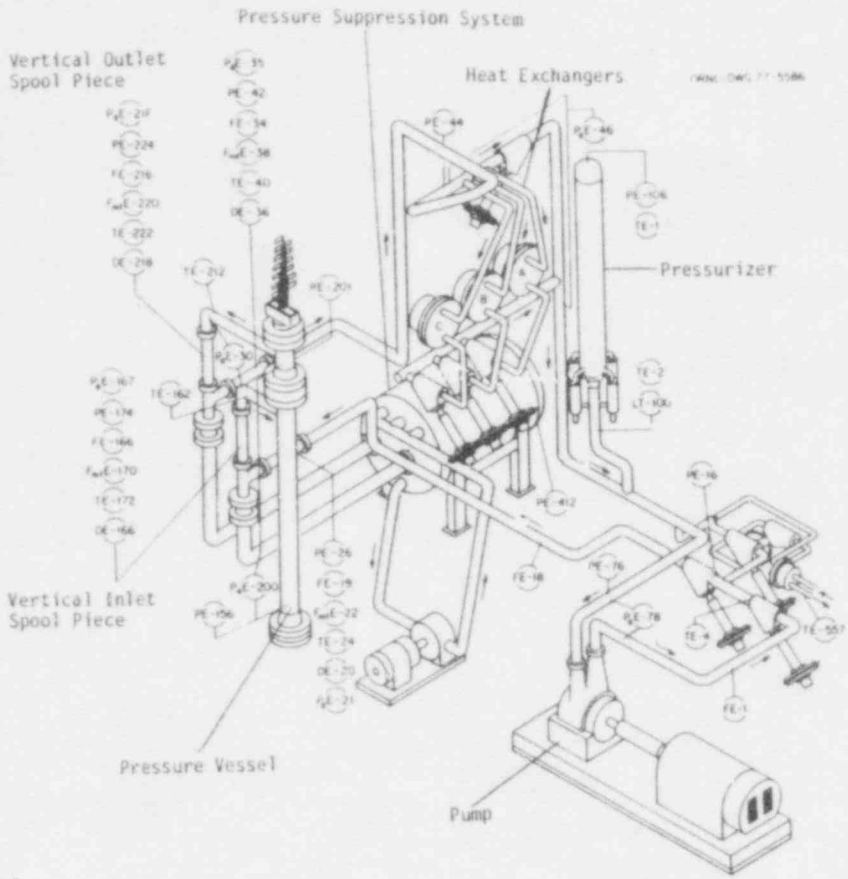

Fig. 1 Schematic of the THTF and instrumentation.

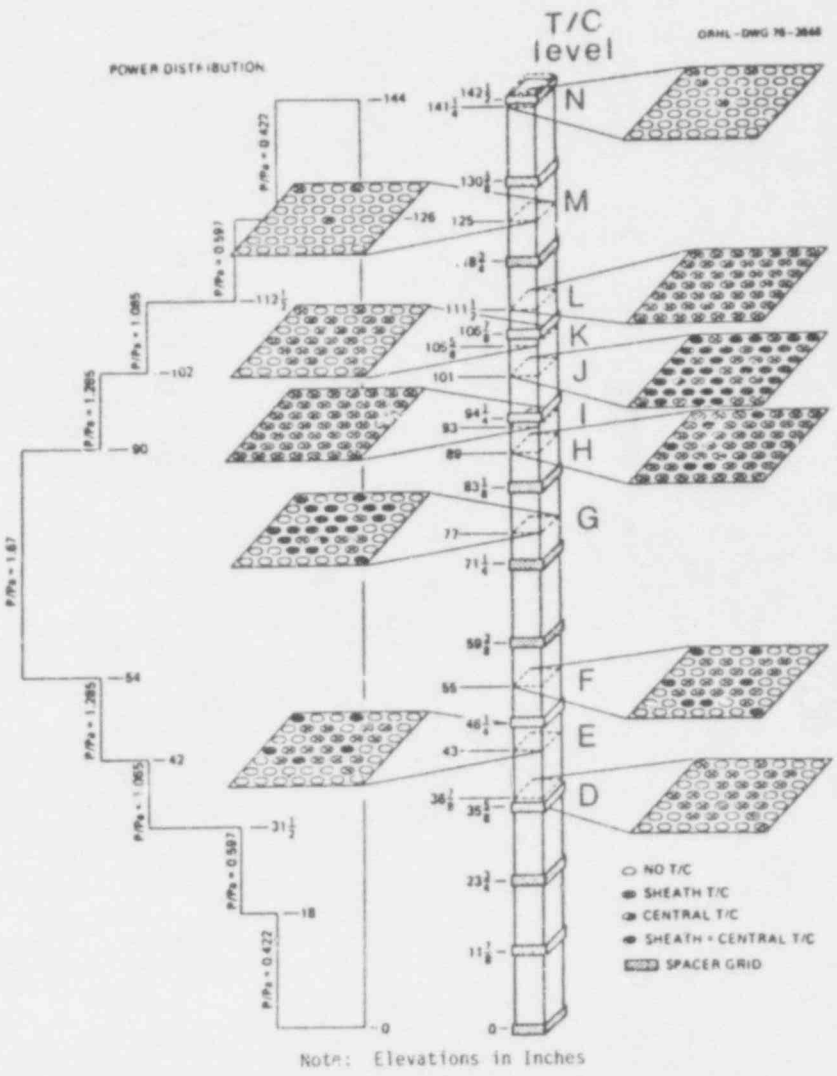

Fig. 2 Thermocouple levels and power steps in the THTF core.

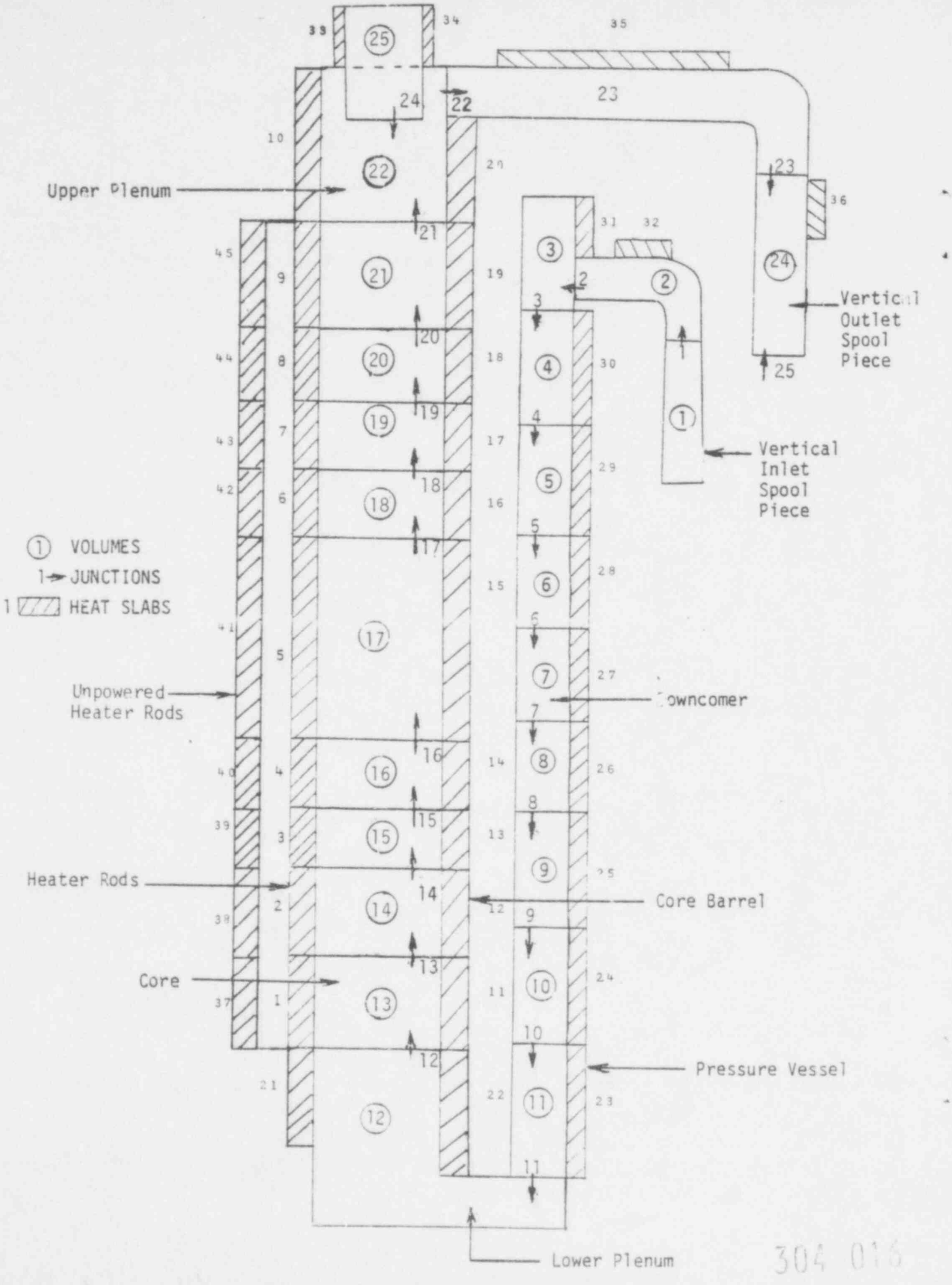

Fig. 3 RELAP4 model of the THTF core.

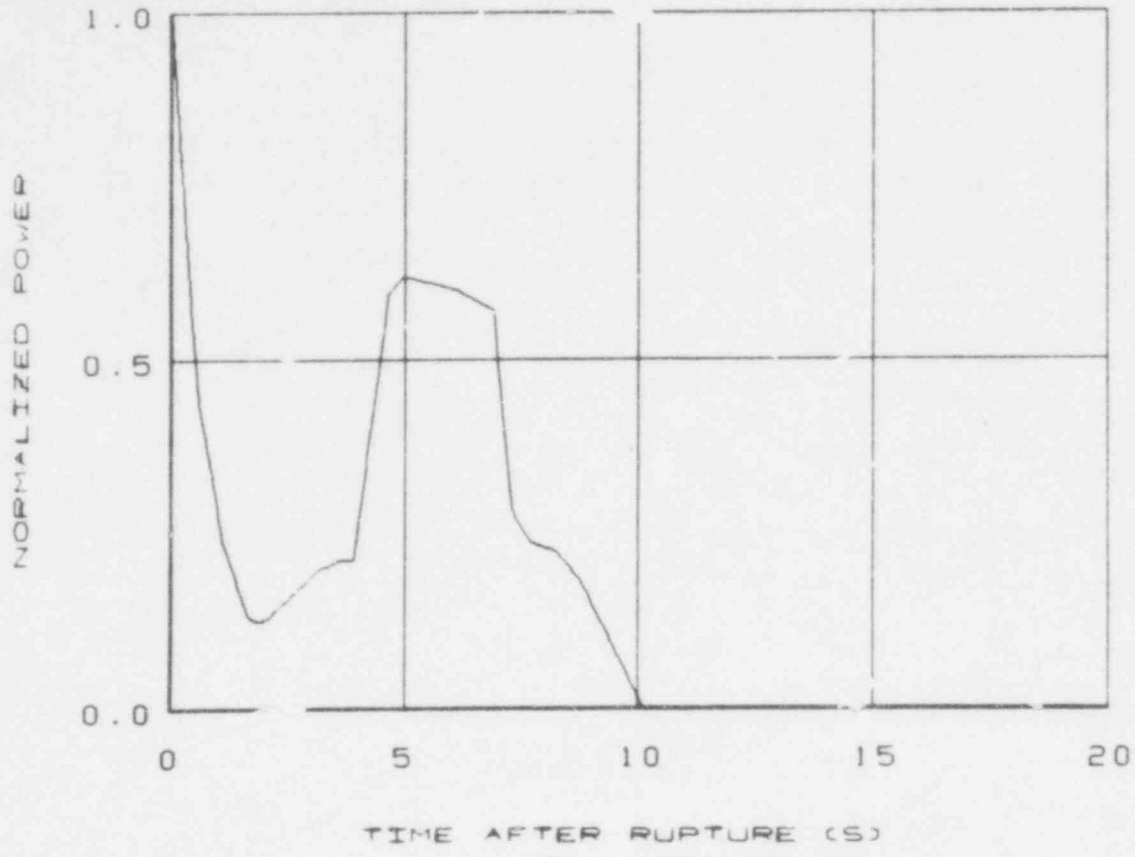

Fig. 4 Test 177 normalized core power history.

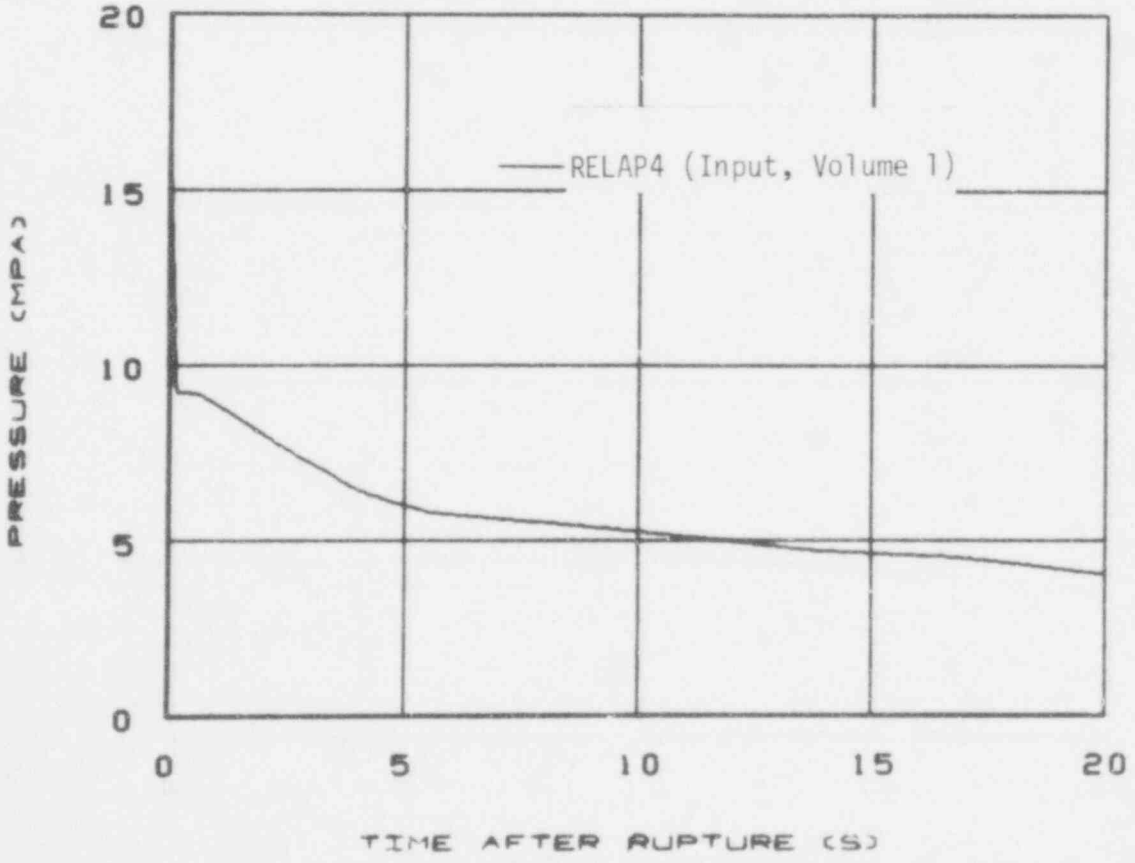

Fig. 5 Fluid pressure in the vertical inlet spool piece.

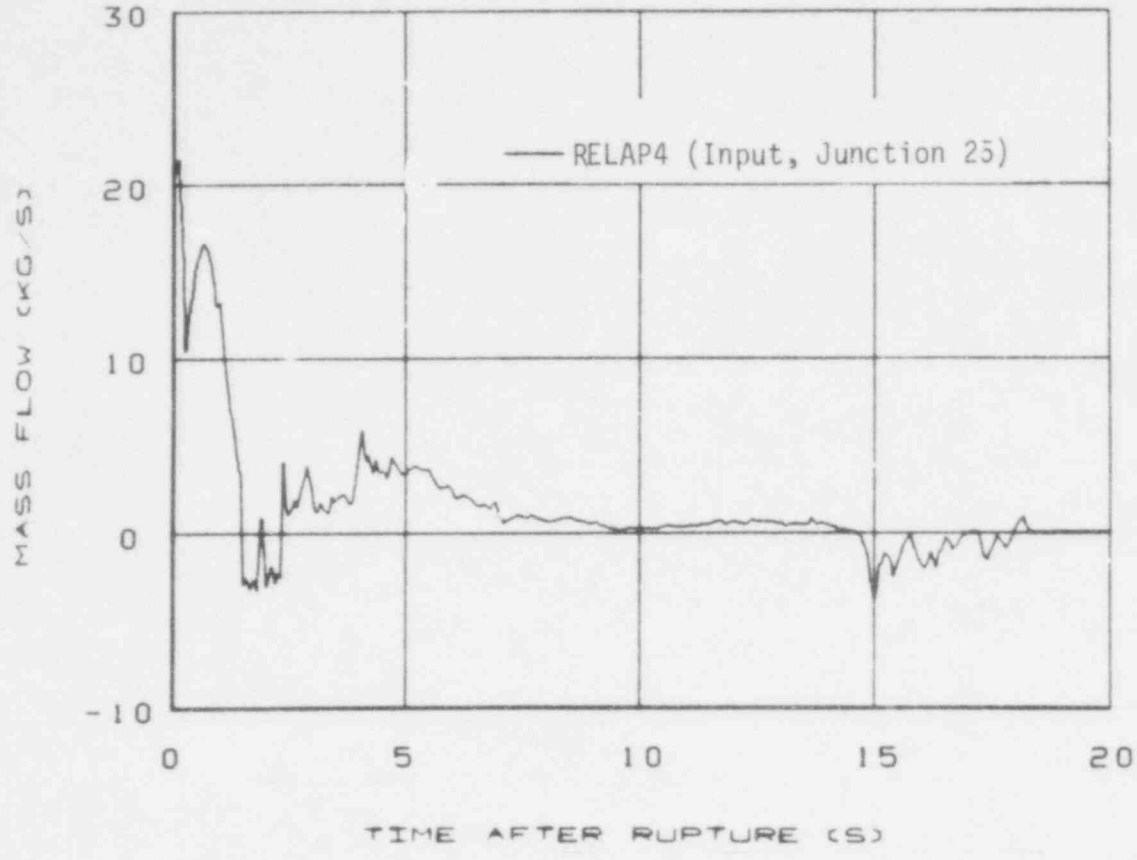

Fig. 6 Fluid mass flow rate in the vertical outlet spool piece.

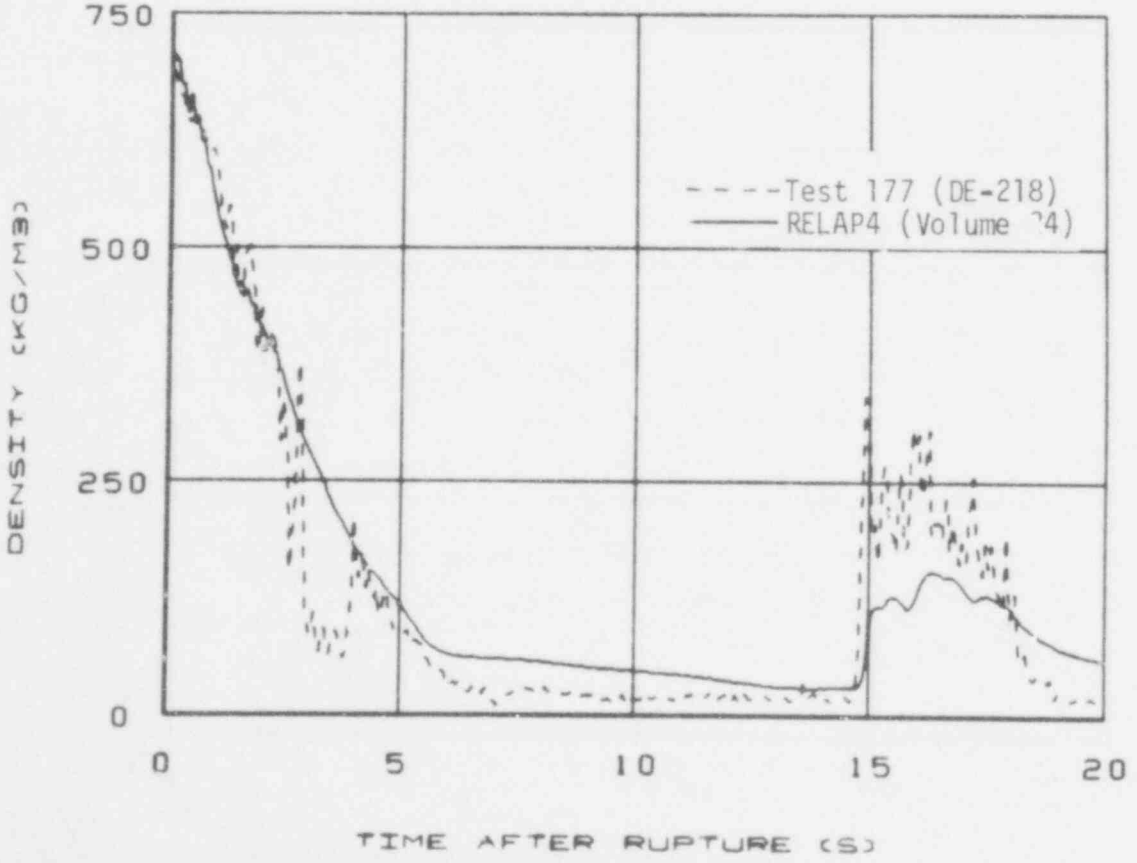

Fig. 7 Fluid density in the vertical outlet spool piece.

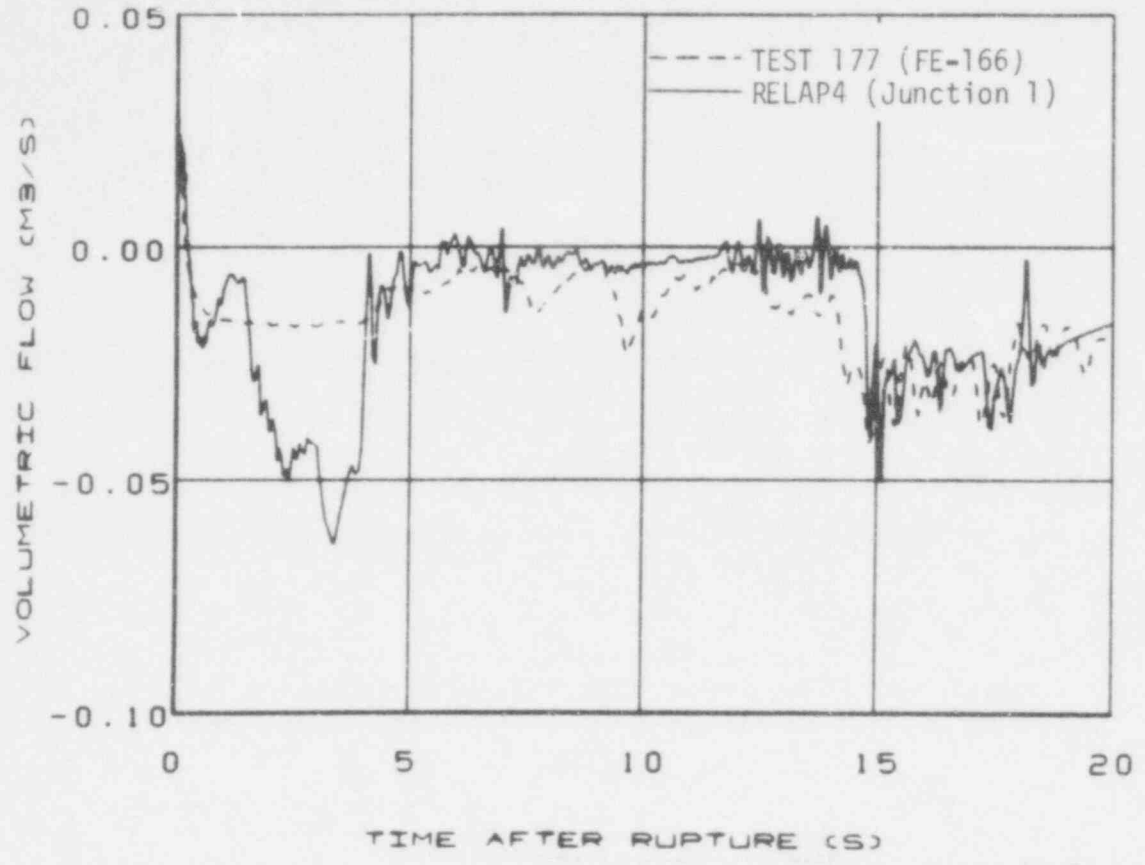

Fig. 8 Fluid volumetric flow rate in the vertical inlet spool piece.

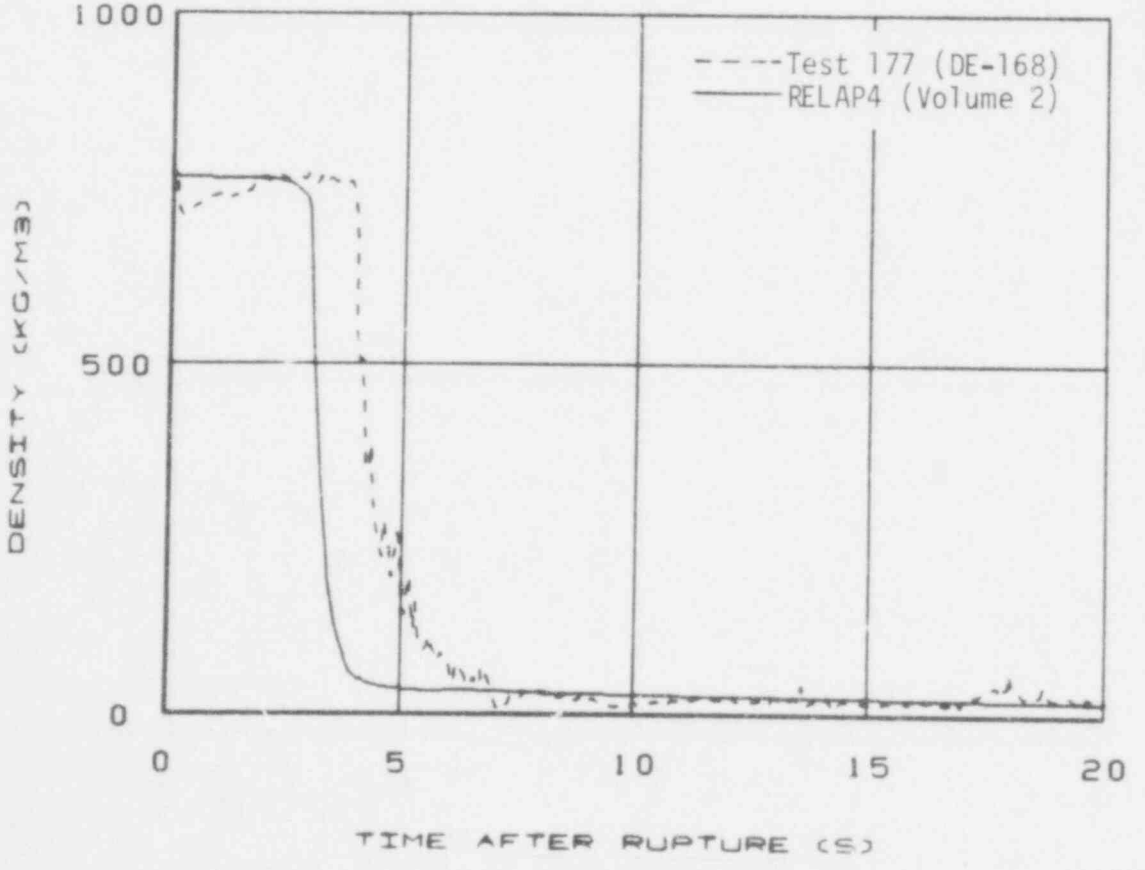

Fig. 9 Fluid density in the vertical inlet spool piece.

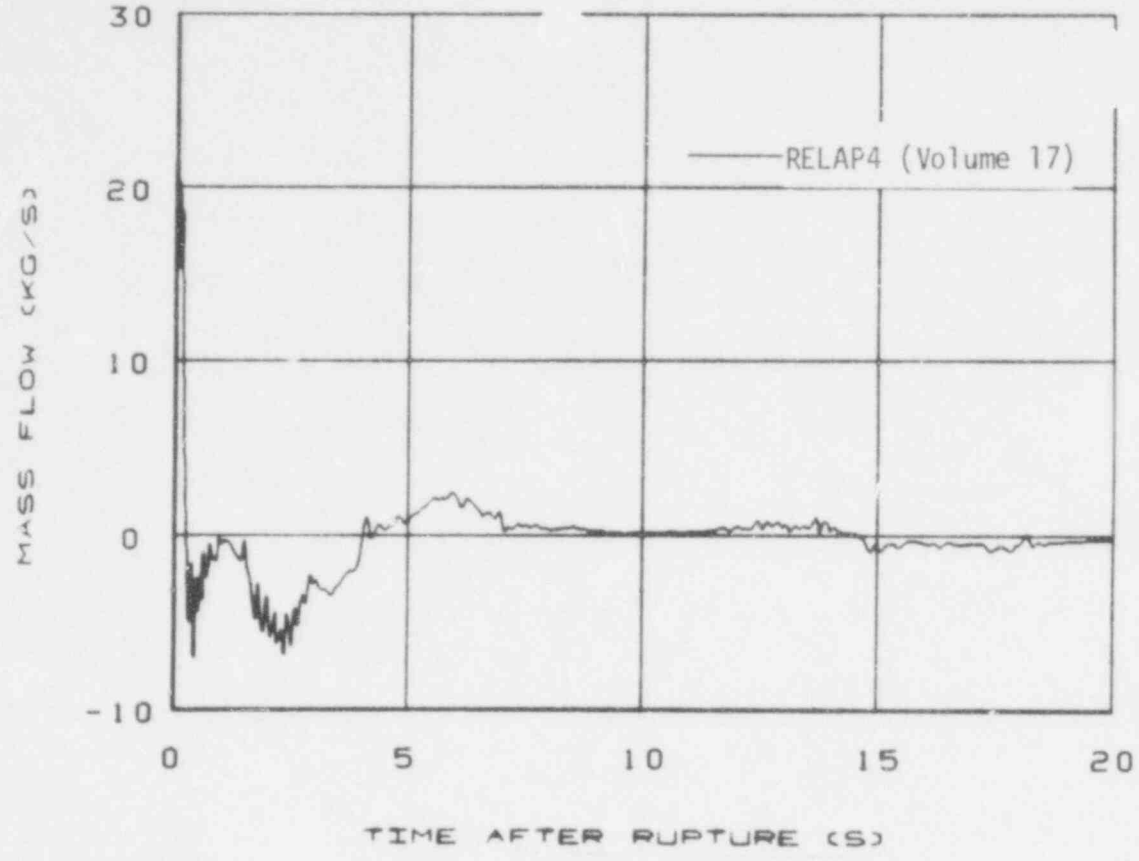

Fig. 10 Mass flow rate in the core.

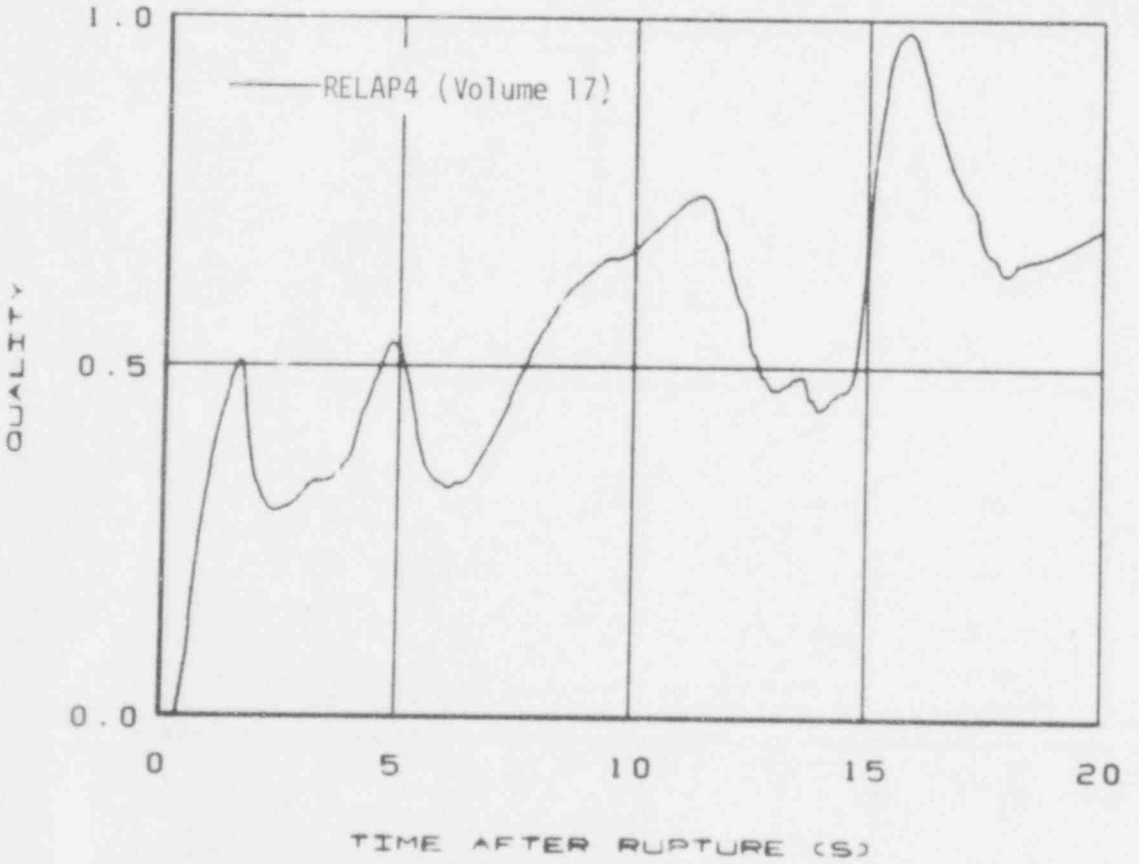

Fig. 11 Fluid quality in the core.

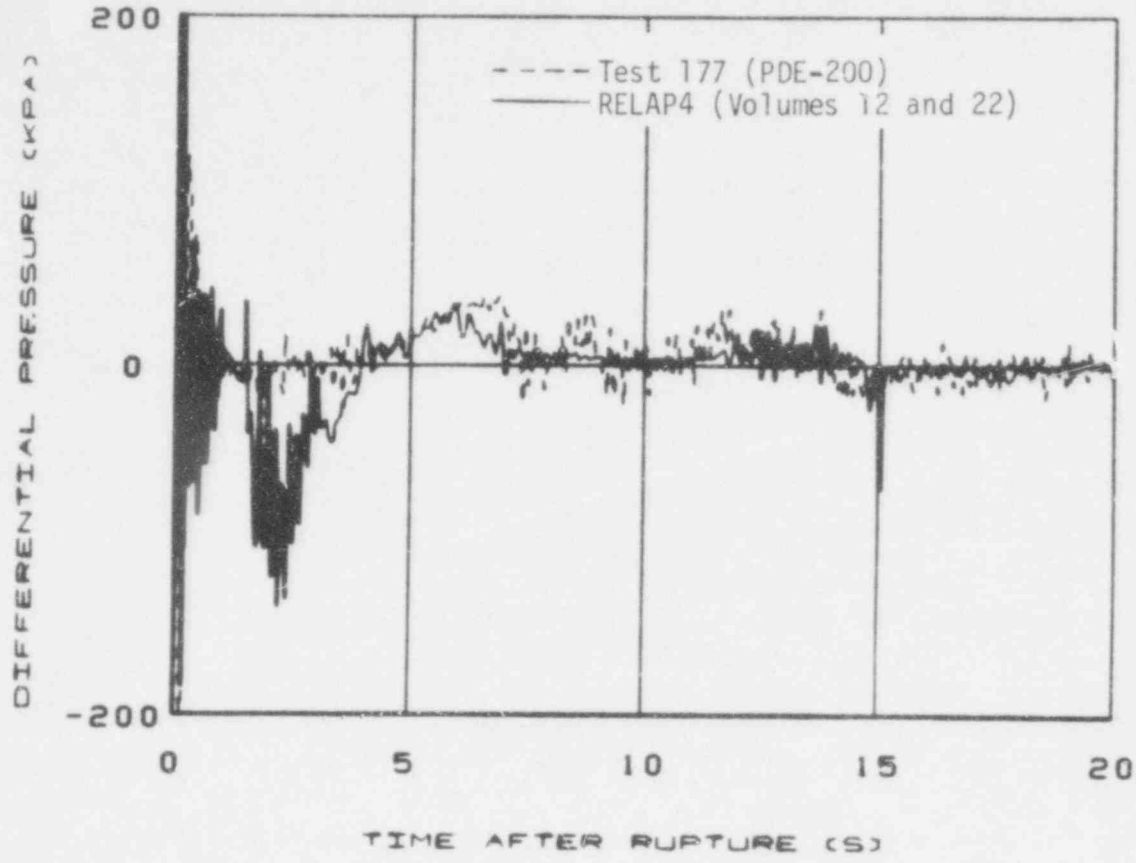

Fig. 12 Differential pressure across the core.

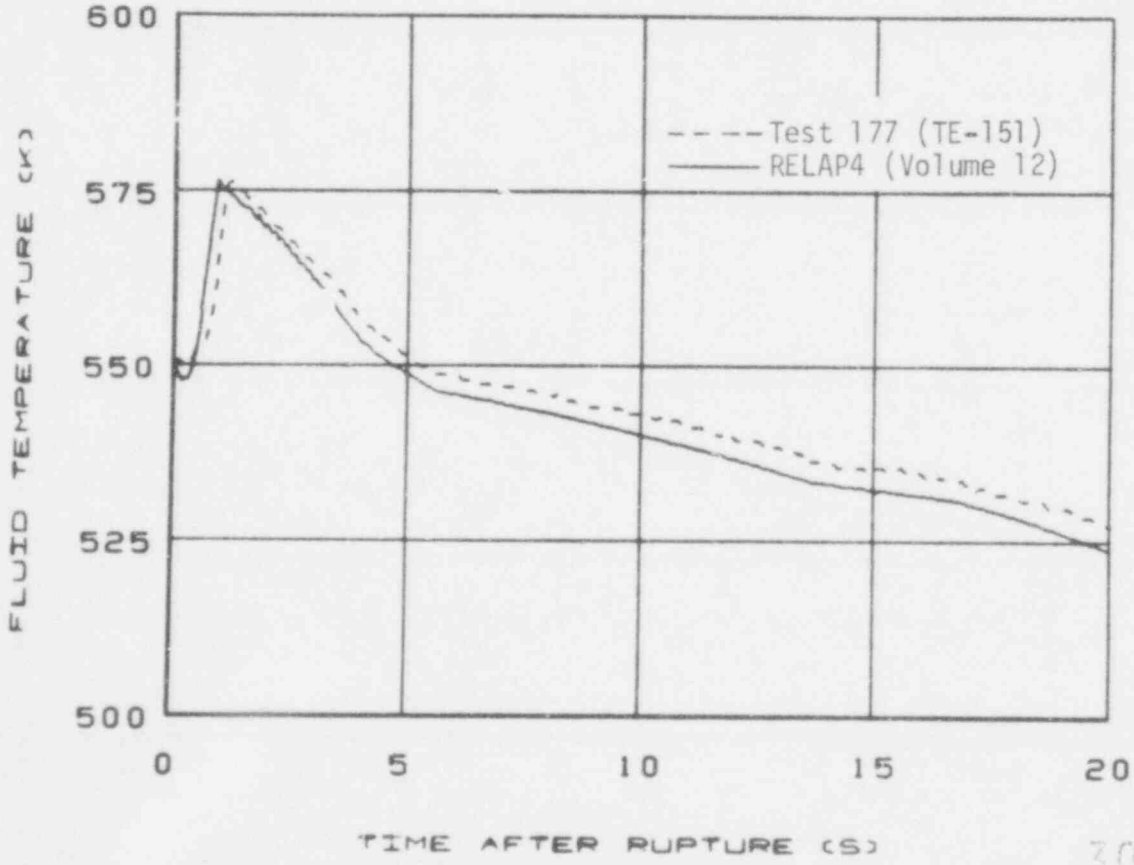

304 021

Fig. 13 Fluid temperature near the bottom of the core.

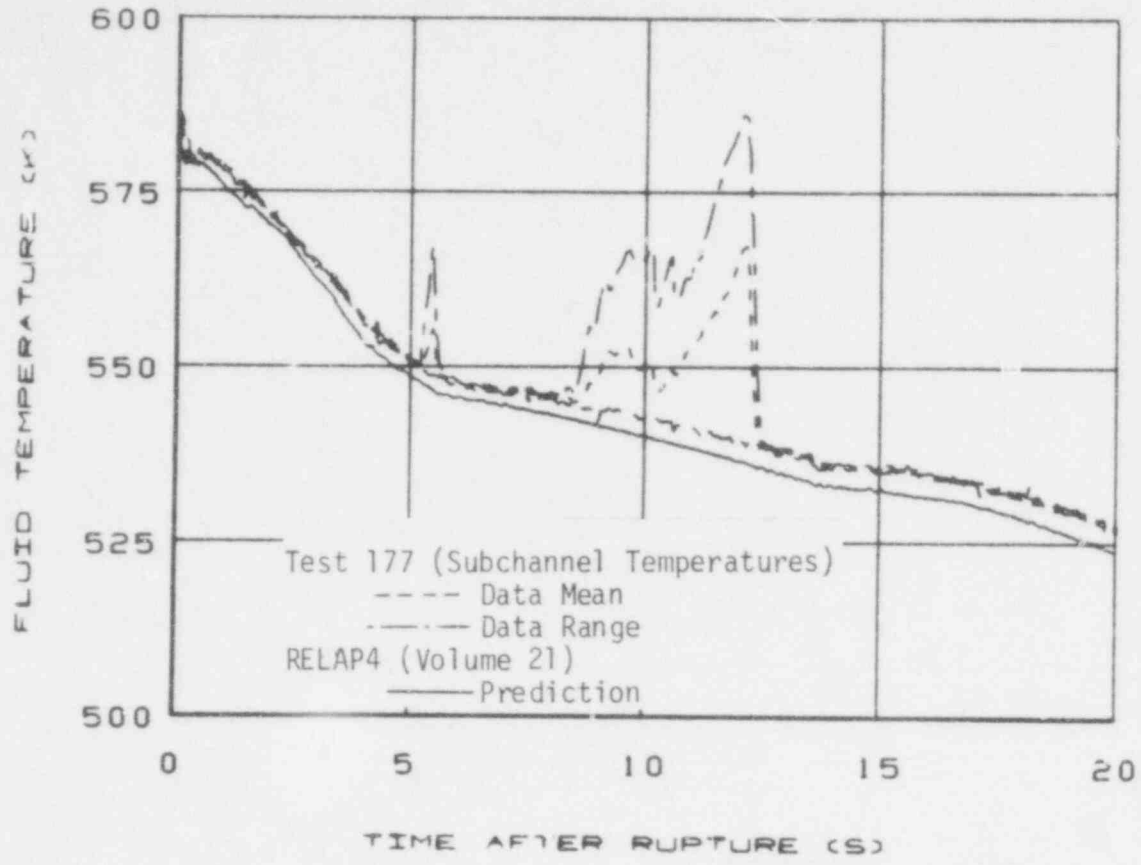

Fig. 14 Fluid temperature near the top of the core.

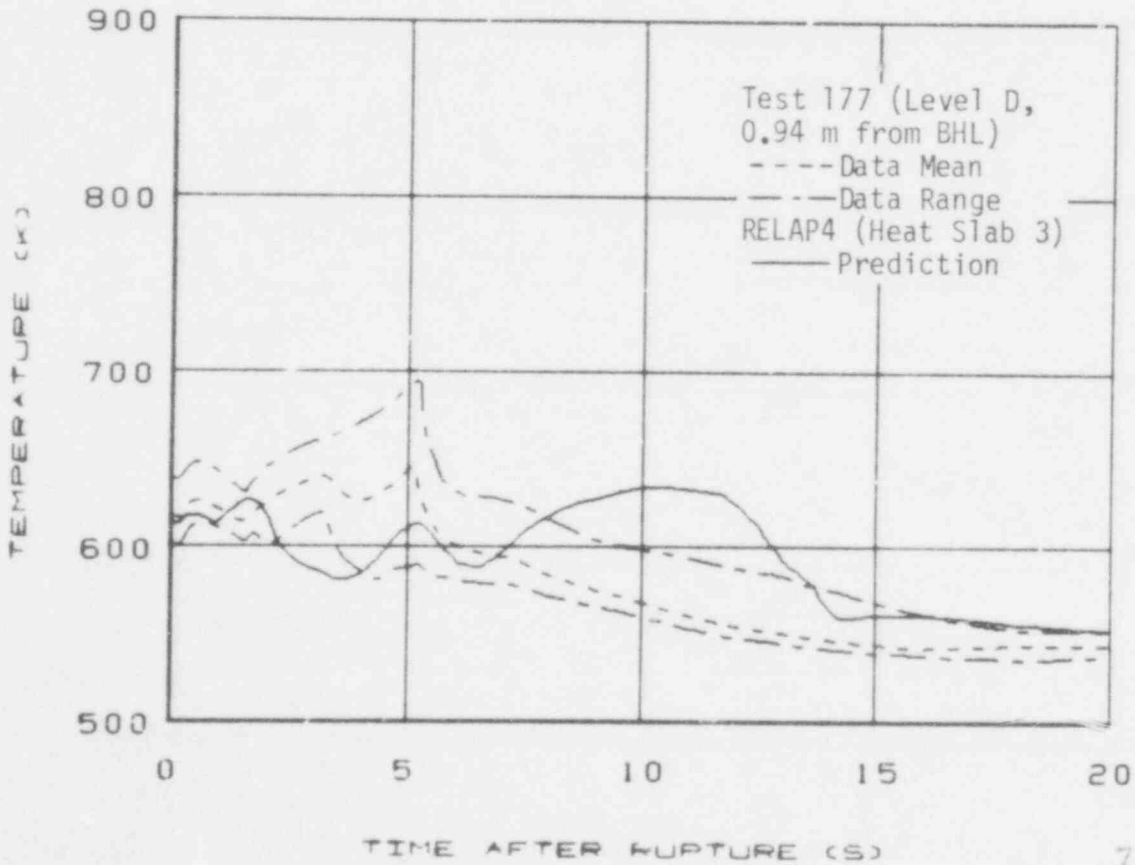

304 022

Fig. 15 Cladding temperature at Level D.

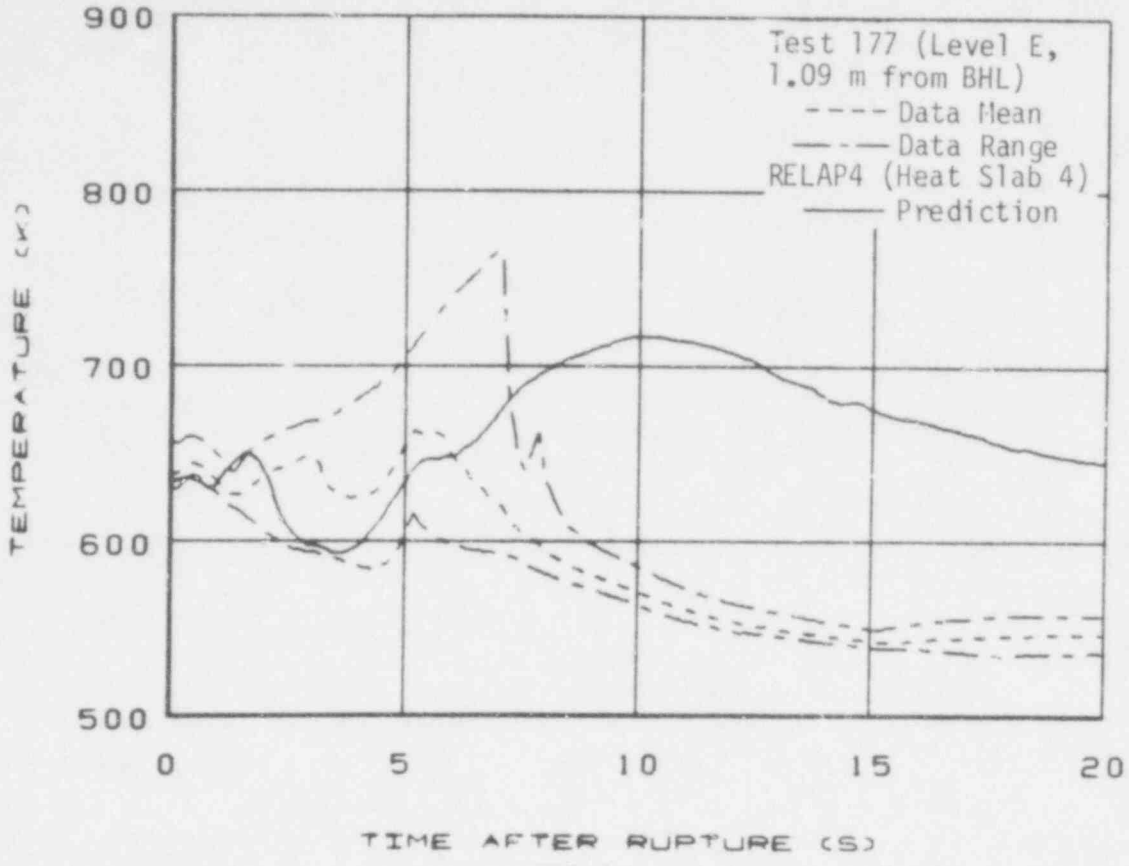

Fig. 16 Cladding temperature at Level E.

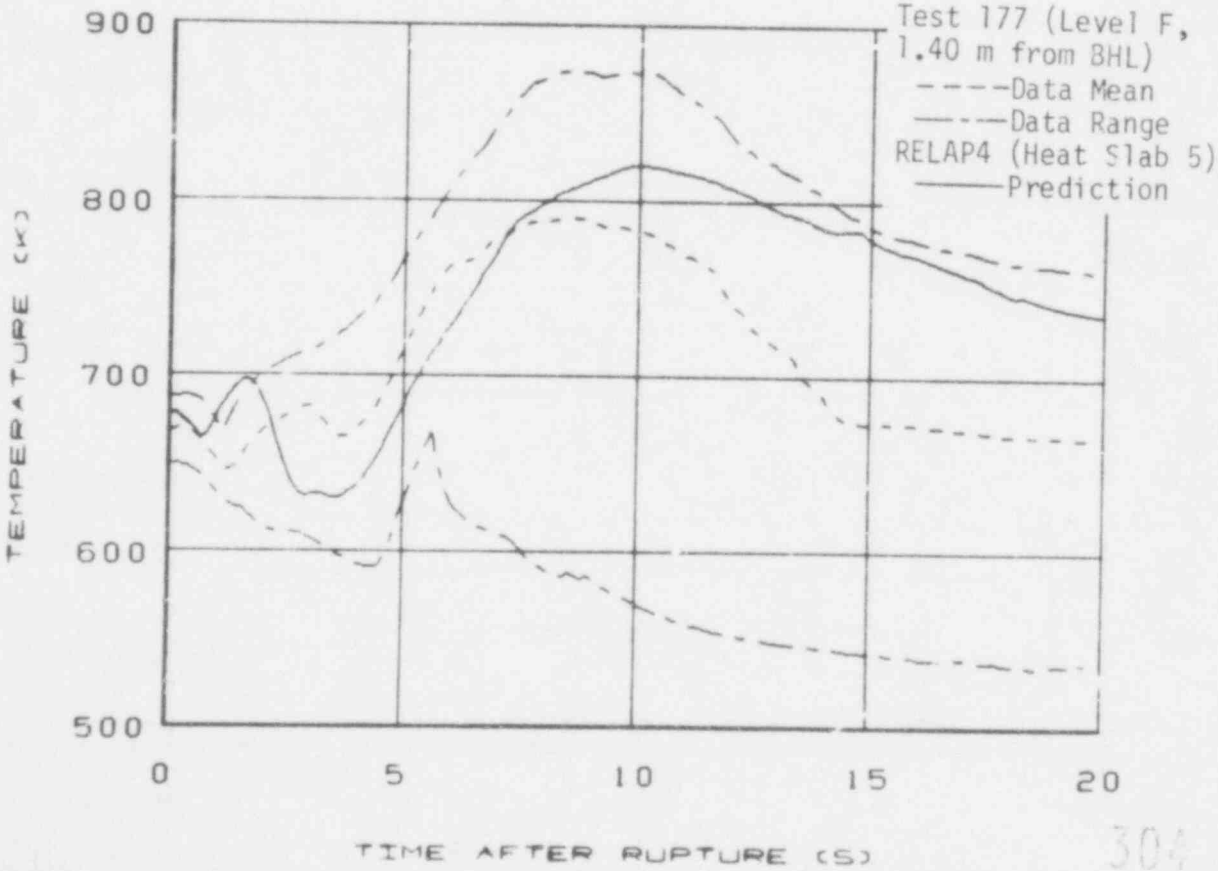

304 023

Fig. 17 Cladding temperature at Level F.

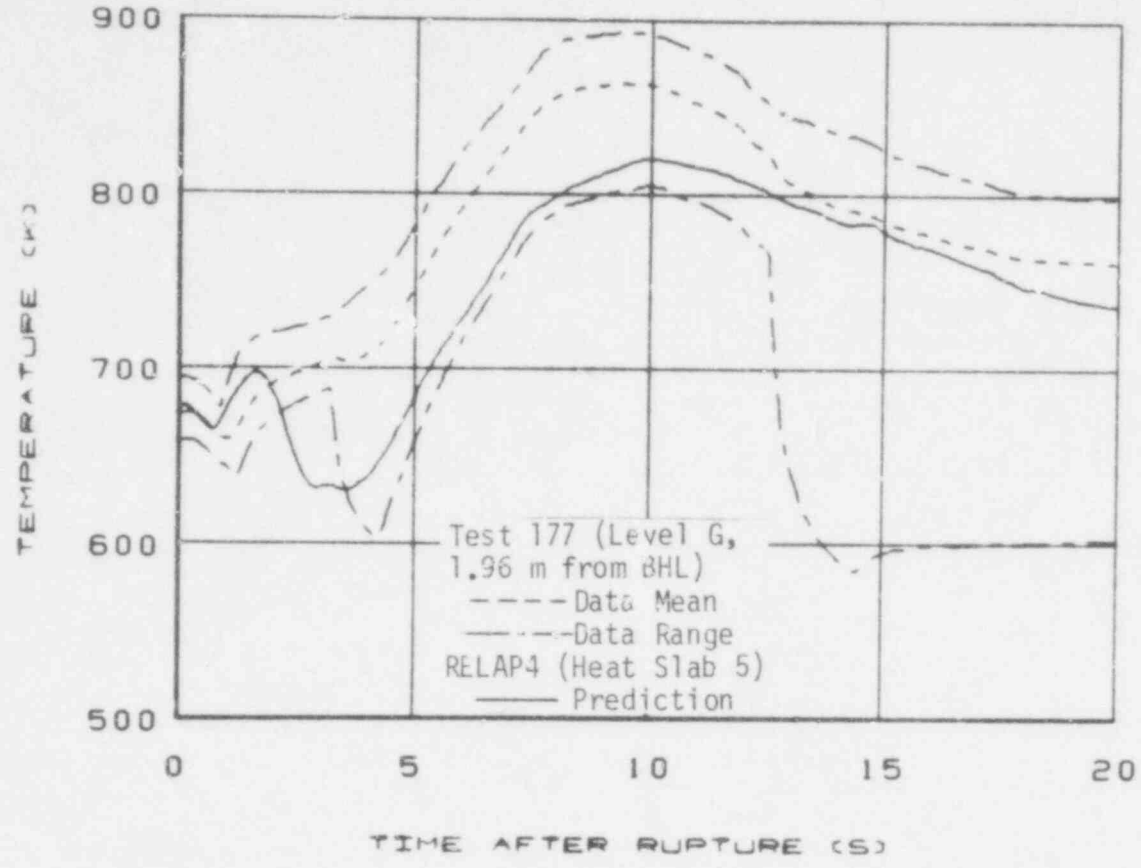

Fig. 18 Cladding temperature at Level G.

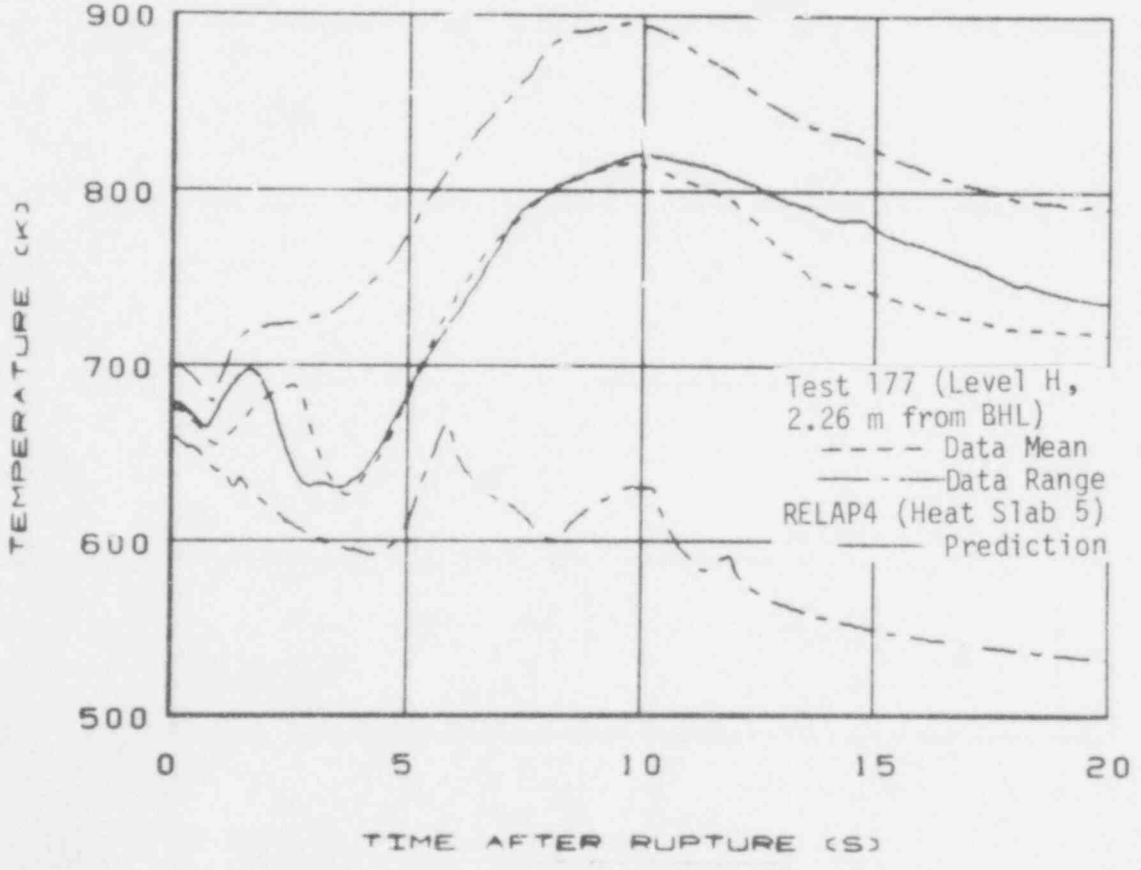

304 024

Fig. 19 Cladding temperature at Level H.

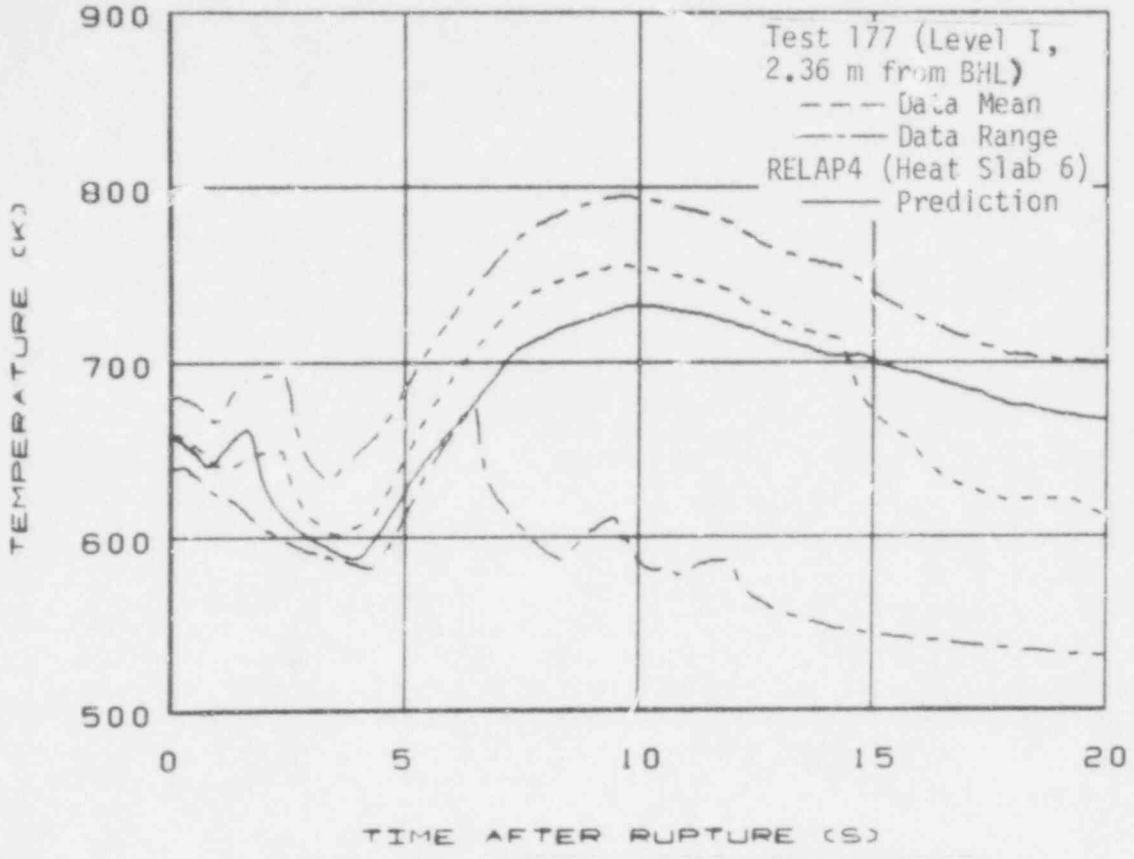

Fig. 20 Cladding temperature at Level I.

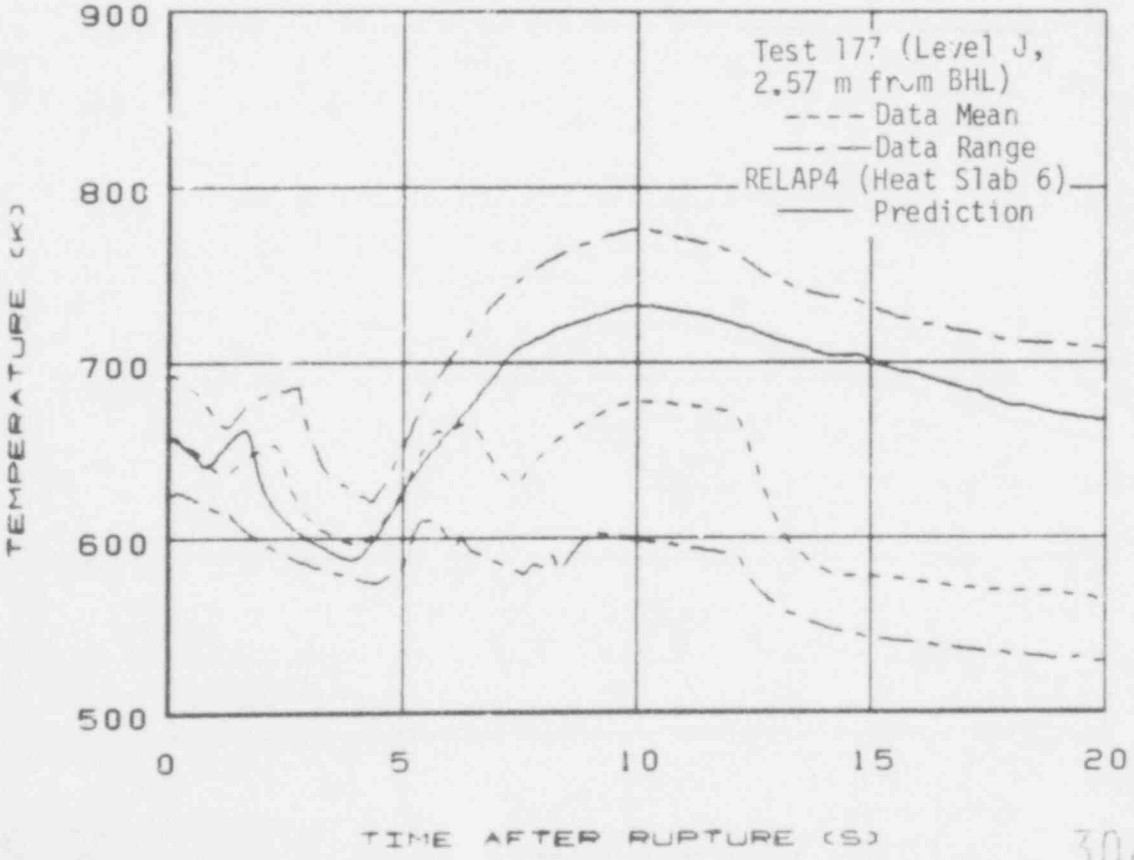

Fig. 21 Cladding temperature at Level J.

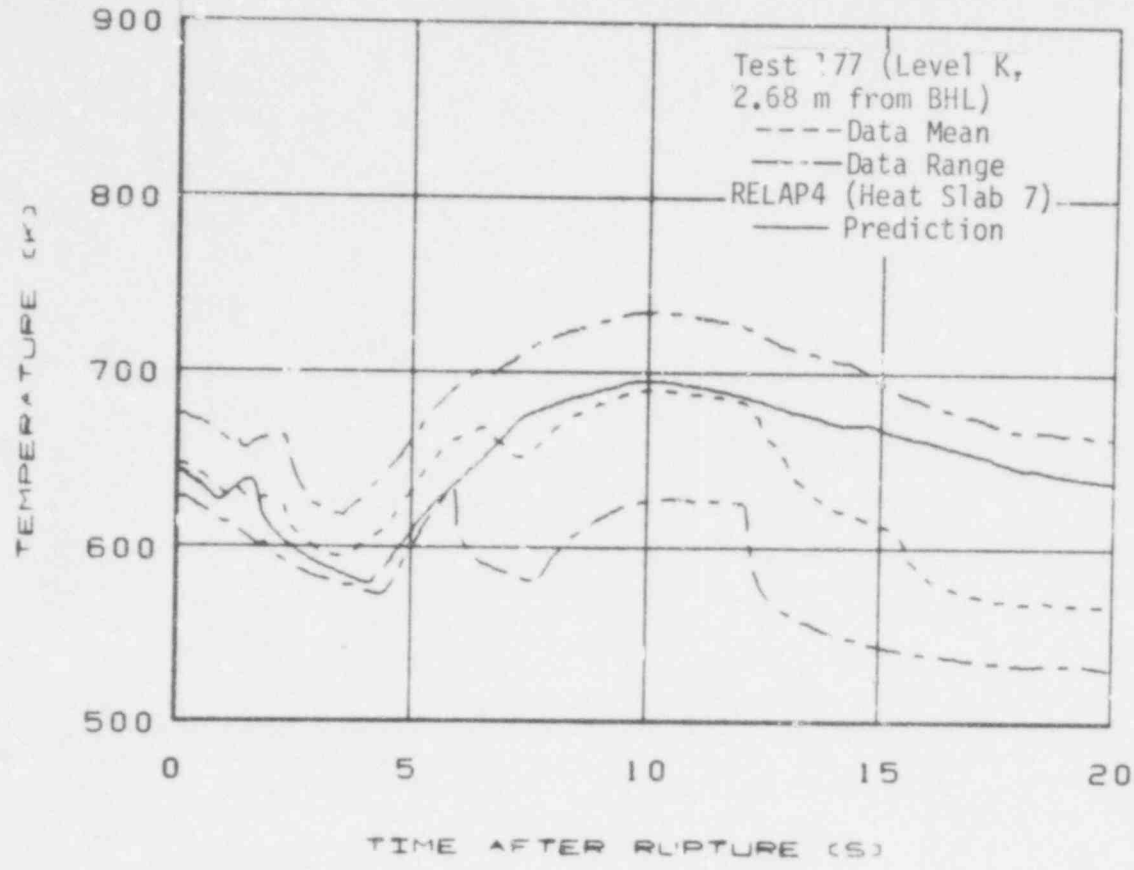

Fig. 22 Cladding temperature at Level K.

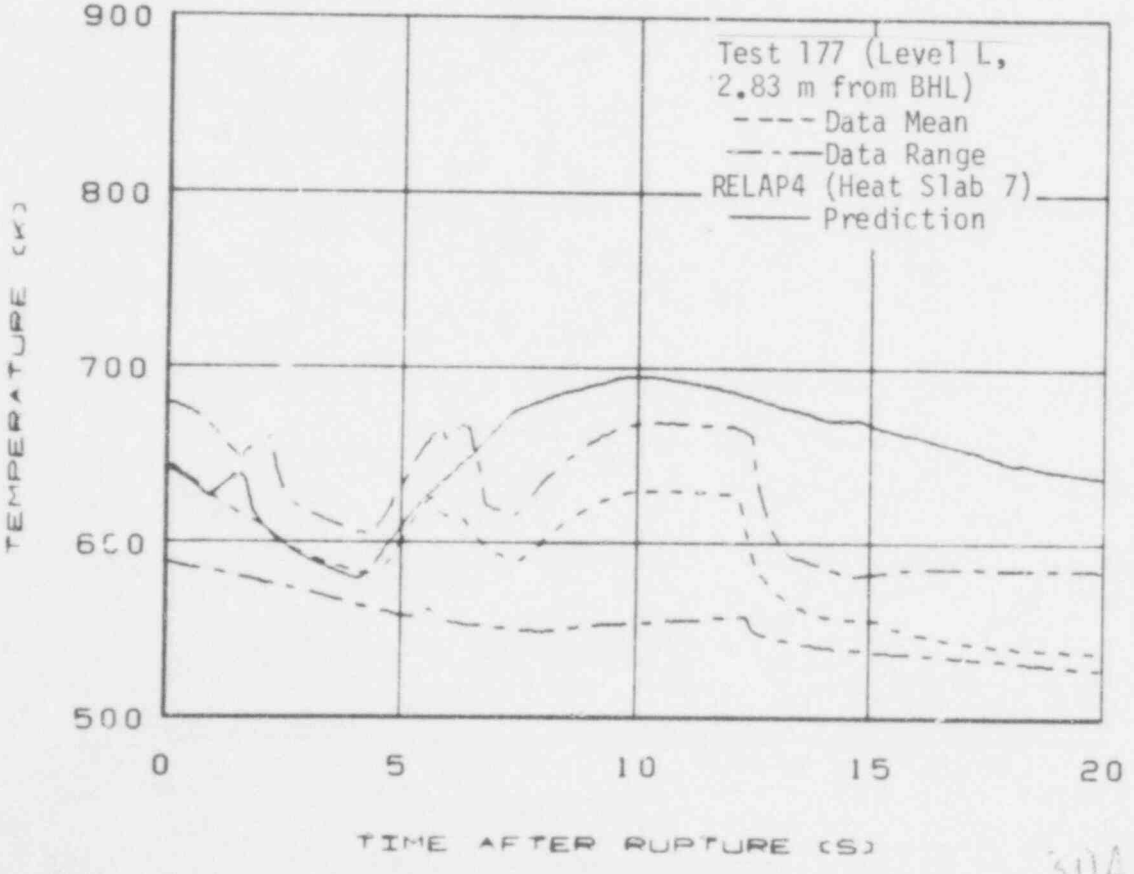

304 026

Fig. 23 Cladding temperature at Level L

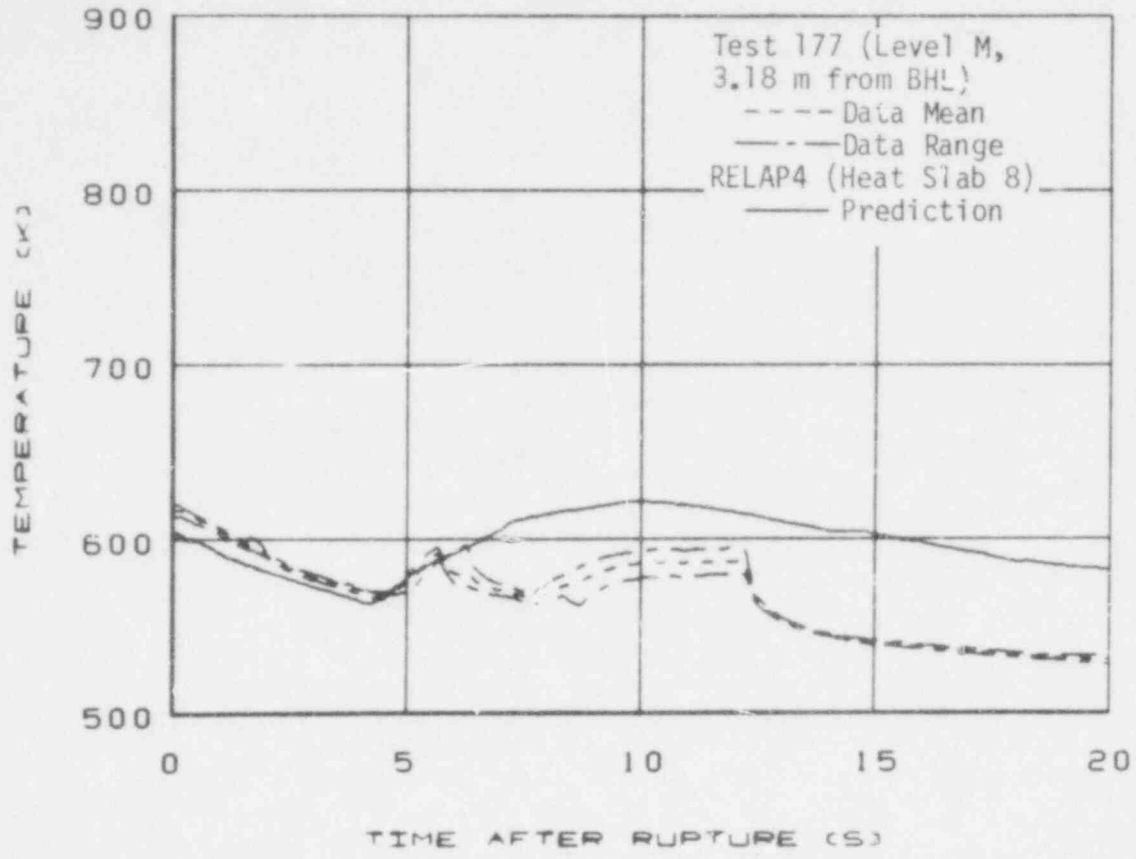

Fig. 24 Cladding temperature at Level M.

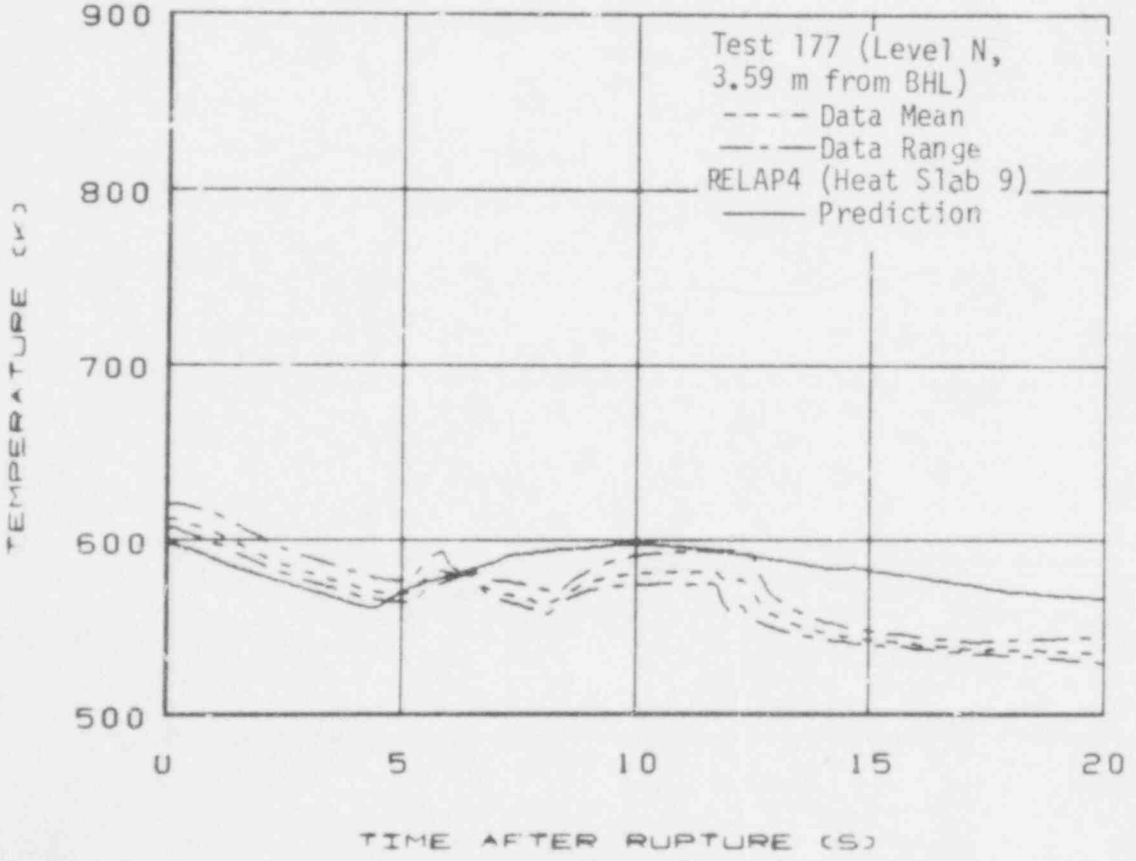

Fig. 25 Cladding temperature at Level N.

304 027

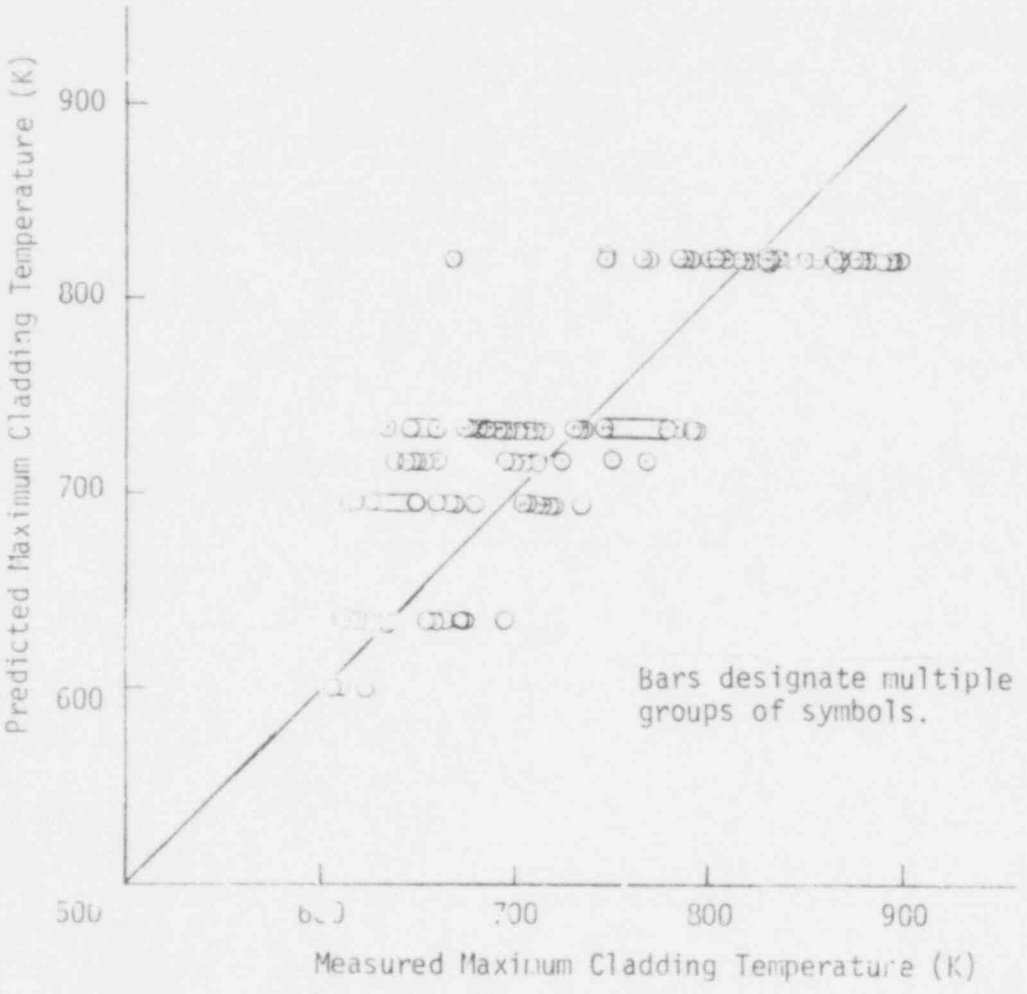

Fig. 26 Predicted vs. measured local maximum cladding temperature.

304 028

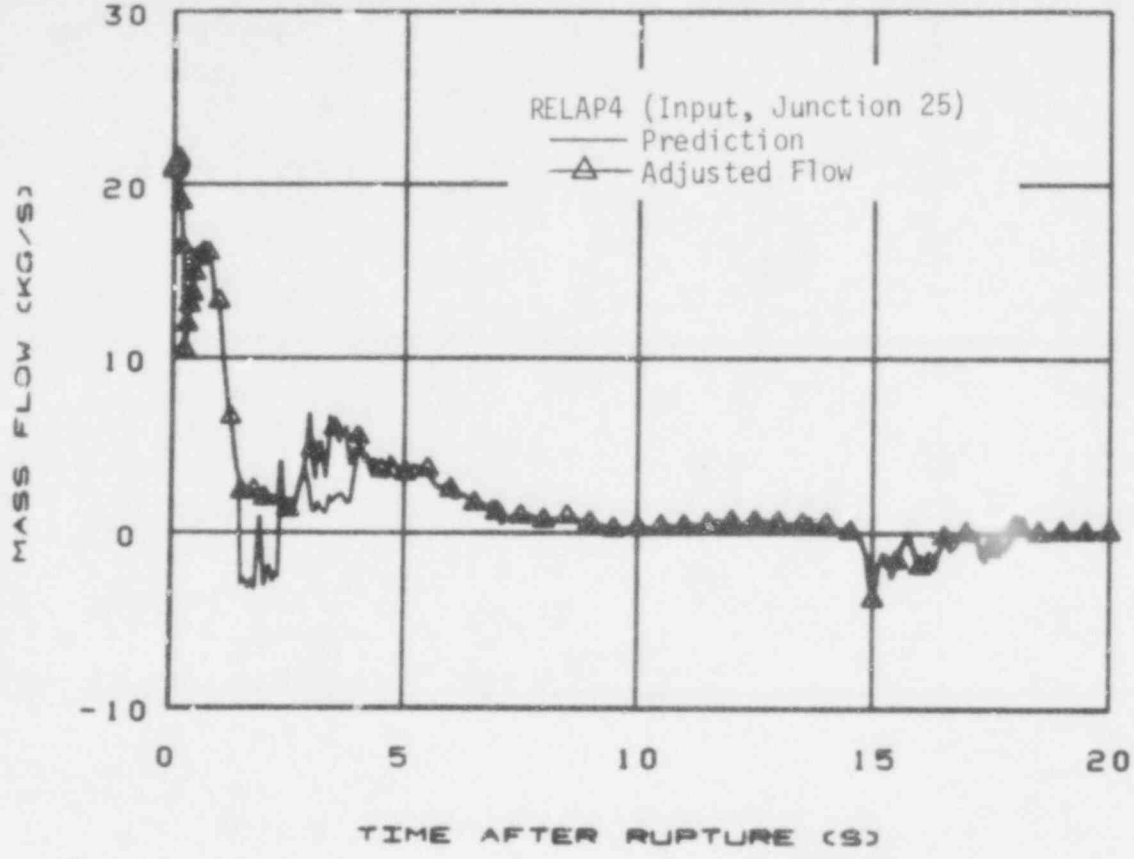

Fig. 27 Fluid mass flow rate in the vertical outlet spool piece.

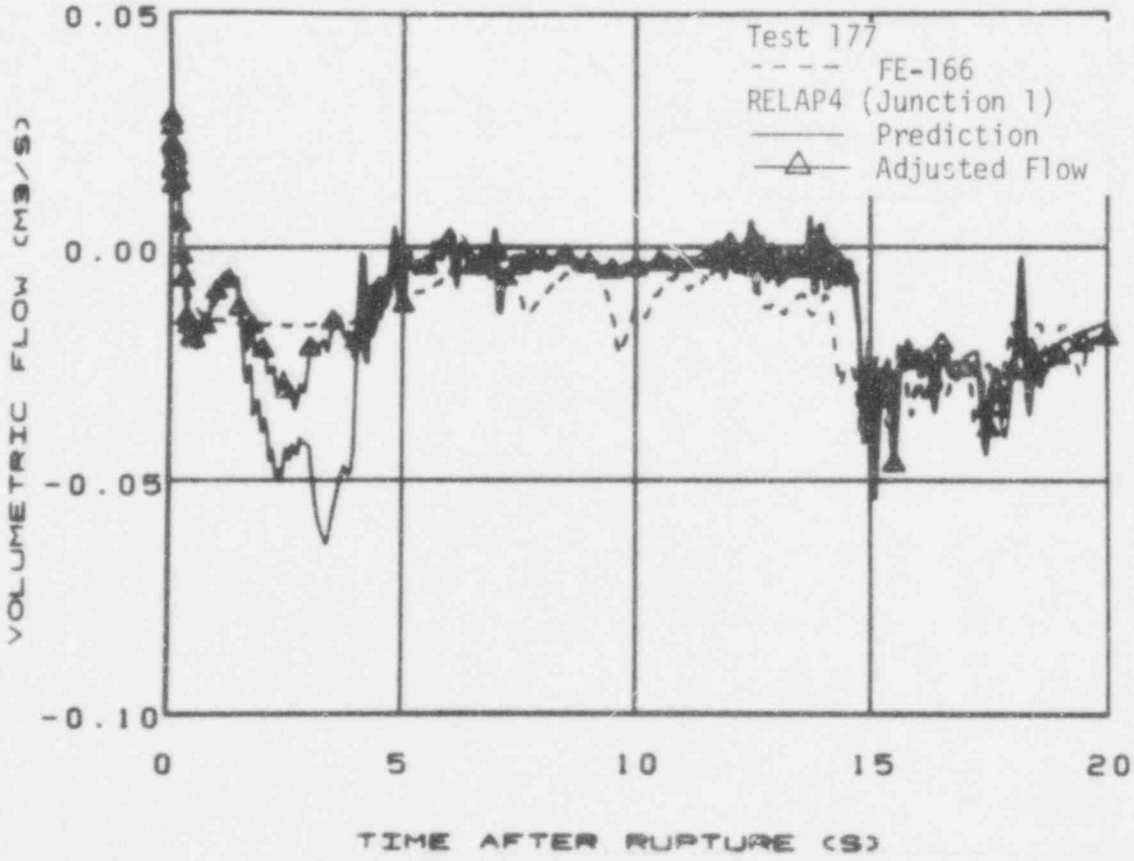

Fig. 28 Fluid volumetric flow rate in the vertical inlet spool piece.

304 029

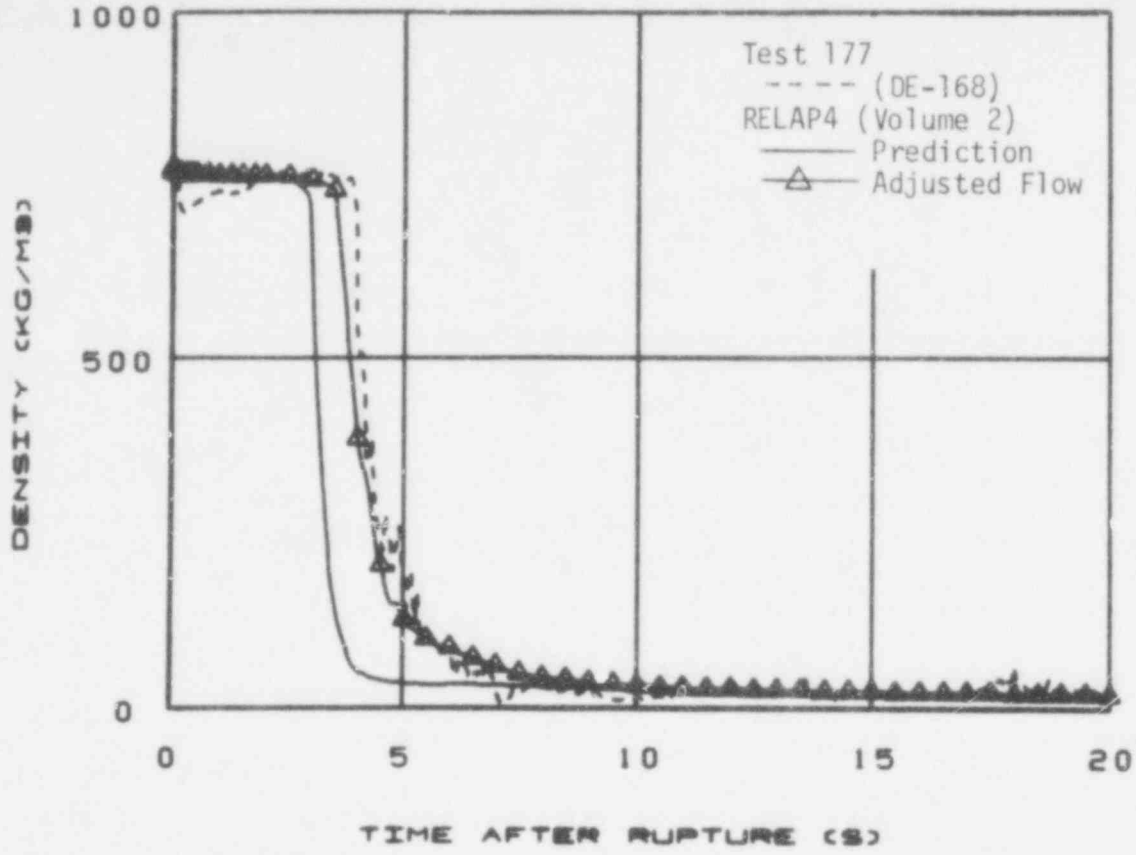

Fig. 29 Fluid density in the vertical inlet spool piece.

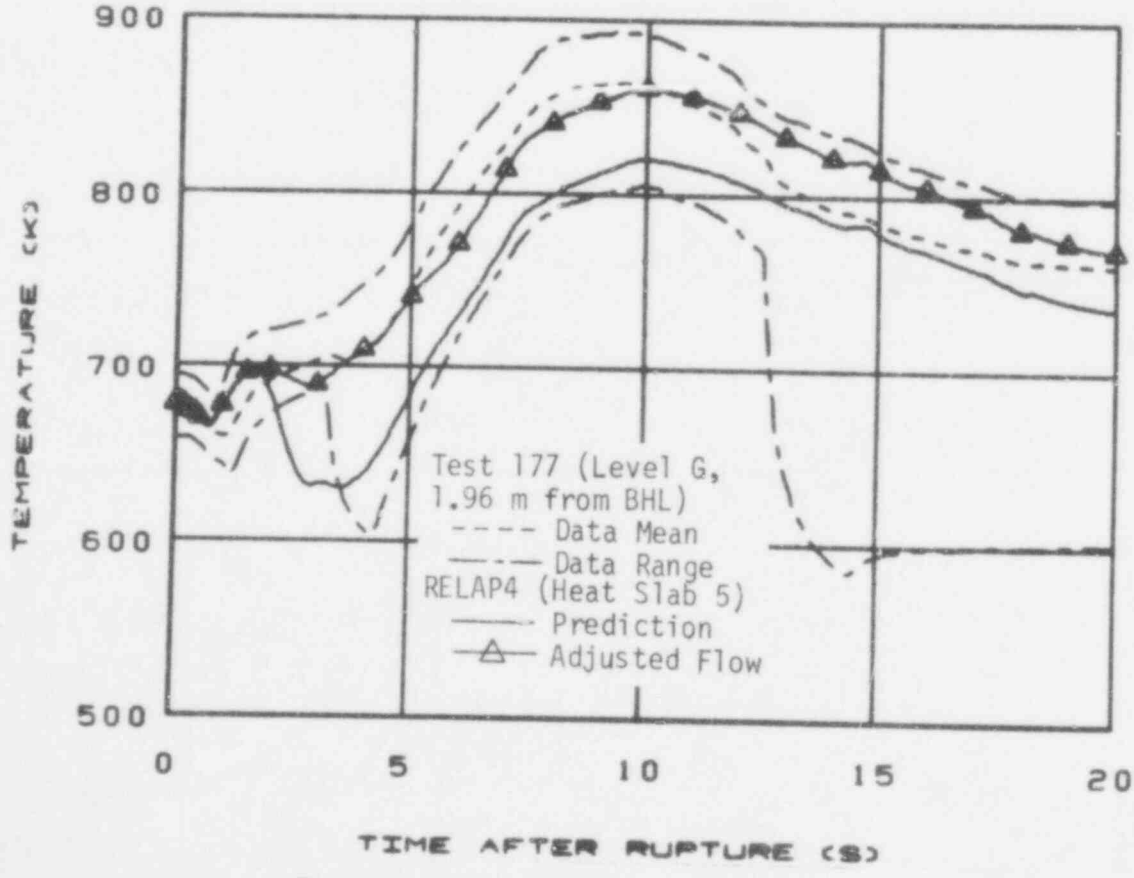

Fig. 30 Cladding temperatures at Level G.

304 030